Annu. Rev. Biomed. Eng. 2000. 02:399–429

TWO-PHOTON EXCITATION FLUORESCENCE MICROSCOPY

Peter T. C. So[1], Chen Y. Dong[1], Barry R. Masters[2], and Keith M. Berland[3]

[1]*Department of Mechanical Engineering, Massachusetts Institute of Technology, Cambridge, Massachusetts 02139; e-mail: ptso@mit.edu*
[2]*Department of Ophthalmology, University of Bern, Bern, Switzerland*
[3]*Department of Physics, Emory University, Atlanta, Georgia 30322*

Key Words multiphoton, fluorescence spectroscopy, single molecule, functional imaging, tissue imaging

■ **Abstract** Two-photon fluorescence microscopy is one of the most important recent inventions in biological imaging. This technology enables noninvasive study of biological specimens in three dimensions with submicrometer resolution. Two-photon excitation of fluorophores results from the simultaneous absorption of two photons. This excitation process has a number of unique advantages, such as reduced specimen photodamage and enhanced penetration depth. It also produces higher-contrast images and is a novel method to trigger localized photochemical reactions. Two-photon microscopy continues to find an increasing number of applications in biology and medicine.

CONTENTS

INTRODUCTION 400
HISTORICAL REVIEW OF TWO-PHOTON MICROSCOPY TECHNOLOGY . . . 401
BASIC PRINCIPLES OF TWO-PHOTON MICROSCOPY 402
Physical Basis for Two-Photon Excitation 402
Optical Properties of Two-Photon Microscopy 403
TWO-PHOTON MICROSCOPY INSTRUMENTATION 404
Two-Photon Laser Sources 404
Scanning Fluorescence Microscopy Optics 405
Fluorescence Detection System 406
FLUORESCENT PROBES USED IN TWO-PHOTON MICROSCOPY 406
Extrinsic and Endogenous Two-Photon Fluorophores 406
Recent Efforts in Two-Photon Probe Development 408
PHYSIOLOGICAL EFFECTS OF NEAR-IR MICROBEAM ILLUMINATION . . . 409
MOLECULAR-LEVEL APPLICATIONS OF TWO-PHOTON MICROSCOPY . . . 410
Single-Molecule Detection in Solution 410
Imaging Single Molecules with Two-Photon Excitation 411

Fluorescence Correlation Spectroscopy 411
Photon-Counting Histogram 413
CELLULAR-LEVEL APPLICATIONS OF TWO-PHOTON MICROSCOPY 414
Two-Photon In Vivo Cellular Imaging—Minimizing Photodamage and Bleaching 414
Multiphoton Imaging of Far-UV Fluorophores 414
Two-Photon Multiple Color Imaging 415
Three-Dimensional Localized Uncaging of Signaling Molecules 415
TISSUE LEVEL APPLICATIONS OF TWO-PHOTON MICROSCOPY 416
Applying Two-Photon Microscopy to Study Tissue Physiology 416
Applying Two-Photon Excitation for Clinical Diagnosis and Treatment 417
NEW DEVELOPMENTS IN TWO-PHOTON INSTRUMENTATION 418
Two-Photon Video Rate Microscopy 418
Simultaneous Two-Photon Fluorescence and Reflected-Light Confocal Microscopy 419
Integrating Fluorescence Spectroscopy into Two-Photon Microscopes 420
CONCLUSION 421

INTRODUCTION

The need for better diagnostic tools has triggered a renaissance in optical-microscopy instrumentation development. Two-photon fluorescence microscopy (TPM), invented by Denk et al in 1990 (1), is a three-dimensional (3D) imaging technology based on the nonlinear excitation of fluorophores. TPM is considered a revolutionary development in biological imaging because of its four unique capabilities. First, TPM greatly reduces photodamage and allows imaging of living specimens. Second, TPM can image turbid specimens with submicrometer resolution down to a depth of a few hundred micrometers. Third, TPM allows high-sensitivity imaging by eliminating the contamination of the fluorescence signal by the excitation light. Fourth, TPM can initiate photochemical reaction within a subfemtoliter volume inside cells and tissues.

This review covers the historical development of two-photon fluorescence microscopy techniques and the underlying physical principles. The basic instrumentation design for TPM is explained. We describe the two-photon absorption properties of a number of commonly used fluorophores and the recent efforts in synthesizing two-photon optimized new probes. To effectively apply this new technique for live specimen imaging, we need to understand two-photon photodamage mechanisms. We discuss a number of biomedical uses of two-photon excitation at the molecular, cellular, and tissue levels. Finally, we survey recent instrumentation development efforts that may lead to more novel applications.

The reader is referred to several previous reviews of topics included in this chapter (2–4). The patent from the Cornell group of Webb and coworkers, which describes multiphoton excitation microscopy, is critical reading (5). An introduction to confocal microscopy and its applications is provided elsewhere (6, 7).

Confocal microscopy is reviewed in a new book of reprinted selected historical papers and patents (8).

HISTORICAL REVIEW OF TWO-PHOTON MICROSCOPY TECHNOLOGY

The potential for highly intense light to trigger nonlinear processes has long been recognized. In particular, multiphoton excitation processes were predicted by Maria Göppert-Mayer in her doctoral dissertation on the theory of two-photon quantum transitions in atoms (9). Experimental work in nonlinear optics may have begun with the work by Franken and his group in 1961, focusing on second harmonic generation of light (10). They showed that ruby laser light, at wavelength λ, propagating through a quartz crystal will generate light at the second harmonic frequency with a wavelength of $\lambda/2$. In 1963, a few weeks after the publication of the paper by Franken et al, Kaiser & Garret published the first report on two-photon excitation (TPE) of CaF_2:Eu^{2+} fluorescence (11). They later demonstrated that TPE also can excite the fluorescence of organic dyes. Since then, many examples of TPE processes in molecular spectroscopy have been reported (12, 13). Two-photon spectroscopy has become an important tool to study the electronic structure of the molecular excited states (14, 15). Göppert-Mayer's theory was finally verified 32 years after its formulation. By analogy with the two-photon processes, three-photon excitation spectroscopy has also been described. Three-photon absorption processes were first reported by Singh & Bradley (16). Since then others have demonstrated three-photon excitation processes (17, 18). Today, the term multiphoton excitation commonly describes two and higher numbers of photon excitation processes.

After the development of nonlinear optical spectroscopy, the potential of nonlinear optical effects in microscopy was soon recognized. In a conventional light microscope, the source of the contrast is the differences in the absorption coefficients and the optical density of the specimens. For nonlinear microscopy, a specimen with a nonlinear optical cross-section will produce higher harmonic light emission under sufficiently intense illumination. The nonlinear harmonic generation is a function of the molecular structure. All materials possess third-order nonlinear susceptibility and higher-order terms; second-order nonlinear susceptibility exists in specimens that have non-centrosymmetric geometry, such as $LiNbO_3$ crystals and some biological specimens. The principle of nonlinear scanning microscopy has been simply explained (6). Practical applications of nonlinear microscopy started with works of Freund & Kopf (18a); they determined the properties of ferroelectric domains by an analysis of the intensity and the angular distribution of the second harmonic generated within the crystals. Hellwarth & Christensen developed a second harmonic microscope to study microstructures in polycrystalline ZnS materials (19). The potential for incorporating nonlinear optical effects in scanning microscopy has been suggested by an Oxford group

(20, 21). They realized that the nonlinear processes are confined to the focal plane of the objective, because the image intensity would depend quadratically on the illumination power. However, the major impact of nonlinear optics in microscopy was not realized until the seminal work of Denk et al (1), who investigated the potential of imaging two-photon excited fluorescence in a scanning microscope with ultrafast pulsed lasers. The use of fluorescence techniques allows specific labeling of biological structures and provides a sensitive means to study biochemical processes such as calcium signaling in cells.

In addition to second- and higher-order harmonic-light generation, microscopes based on other nonlinear optical effects, such as sum frequency generation, coherent anti-Stoke Raman scattering, and parametric oscillations, have also been considered and implemented [see recent works (22–24)]. The potential of using these newer techniques for biological and medical research still requires further evaluation and is not covered in this review.

BASIC PRINCIPLES OF TWO-PHOTON MICROSCOPY

Physical Basis for Two-Photon Excitation

TPE of molecules is a nonlinear process involving the absorption of two photons whose combined energy is sufficient to induce a molecular transition to an excited electronic state. A comparison between one- and two-photon absorption is shown in Figure 1 (see color insert). Conventional one-photon techniques use UV or visible light to excite fluorescent molecules of interest. Excitation occurs when the absorbed photon energy matches the energy gap between the ground and excited states. The same transition can be excited by a two-photon process in which two less energetic photons are simultaneously absorbed. Quantum mechanically, a single photon excites the molecule to a virtual intermediate state, and the molecule is eventually brought to the final excited state by the absorption of the second photon.

The theory of TPE was predicted by Göppert-Mayer in 1931 (9). The basic physics of this phenomenon has also been described elsewhere (25, 26). Fluorescence excitation is an interaction between the fluorophore and an excitation electromagnetic field. This process is described by a time-dependent Schroedinger equation, in which the Hamiltonian contains an electric dipole interaction term: $\vec{E}_\gamma \cdot \vec{r}$, where $\vec{E}_\gamma$ is the electric field vector of the photons and $\vec{r}$ is the position operator. This equation can be solved by perturbation theory. The first-order solution corresponds to the one-photon excitation (OPE), and the multiphoton transitions are represented by higher order solutions. In the case of TPE, the transition probability between the molecular initial state $|i\rangle$ and the final state $|f\rangle$ is given by

$$P \sim \left| \sum_m \frac{\langle f | \vec{E}_\gamma \cdot \vec{r} | m \rangle \langle m | \vec{E}_\gamma \cdot \vec{r} | i \rangle}{\varepsilon_\gamma - \varepsilon_m} \right|^2 \quad (1)$$

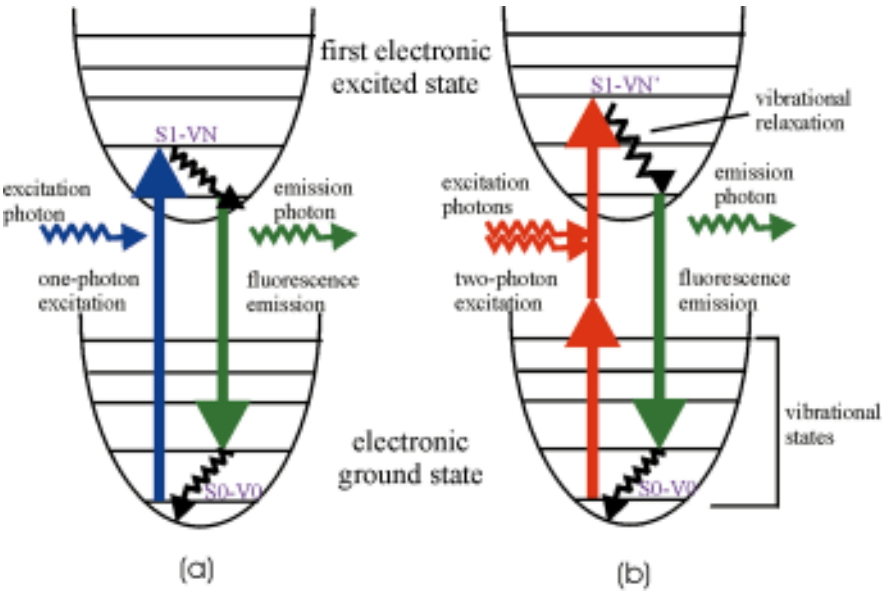

Figure 1 Jablonski diagram for one-photon (*a*) and two-photon (*b*) excitation. Excitations occur between the ground state and the vibrational levels of the first electronic excited state. One-photon excitation occurs through the absorption of a single photon. The initial (*S*0-*V*0) and final (*S*1-*V*N) states have opposite parity. Two-photon excitation occurs through the absorption of two lower-energy photons via short-lived intermediate states. The initial (*S*0-*V*0) and final (*S*1-*VN′*) states have the same parity. After either excitation process, the fluorophore relaxes to the lowest energy level of the first excited electronic states via vibrational processes. The subsequent fluorescence emission processes for both relaxation modes are the same.

where ε_γ is the photonic energy associated with the electric field vector $\vec{E}_\gamma$, the summation is over all intermediate states m, and ε_m is the energy difference between the state m and the ground state. Note that the dipole operator has odd parity (i.e. absorbing one photon changes the parity of the state), and the one-photon transition moment $\langle f|\vec{E}_\gamma \cdot \vec{r}|i\rangle$ dictates that the initial and final states have opposite parity. The two-photon moment $\langle f|\vec{E}_\gamma \cdot \vec{r}|m\rangle\langle m|\vec{E}_\gamma \cdot \vec{r}|i\rangle$ allows transition in which the two states have the same parity (25, 26).

Optical Properties of Two-Photon Microscopy

In TPE microscopy, a high numerical aperture objective is used to focus the excitation source to a diffraction-limited spot. The characteristic spatial profile at the focal plane for a circular lens with $NA = \sin(\alpha)$, focusing light of wavelength λ, is

$$I(u, v) = \left| 2 \int_0^1 J_0(v\rho) e^{-\frac{i}{2}u\rho^2} \rho \, d\rho \right|^2 \quad (2)$$

where J_0 is the zeroth-order Bessel function, $u = 4k \sin^2(\alpha/2)z$, and $v = k \sin(\alpha)r$ are the respective dimensionless axial and radial coordinates normalized to wave number $k = 2\pi/\lambda$ (27, 28). Because TPE depends on the square of incident photon flux, the point spread function (PSF), which represents the geometry of the excitation volume, is $I^2(u/2, v/2)$. Compared with the conventional one-photon PSF, $I(u, v)$, the two-photon result has several major differences leading to distinct advantages for bioimaging applications.

Three-Dimensional Localization of the Excitation Volume A key feature of TPM is the limitation of fluorescence excitation to within a femtoliter size focal volume. Equation 1 indicates that the excitation probability is proportional to the square of laser intensity. The nonlinear feature of excitation implies that two-photon–induced absorption occurs most strongly near the focal plane, where the photon flux is highest (Figure 2; see color insert). Figure 3 (see color insert) compares the radial and axial PSF for one-photon microscopy and TPM. Note that TPE wavelength is twice that of the one-photon case. Owing to the longer wavelength used, TPM has a wider PSF when compared with the one-photon case. On the other hand, the true strength of TPM is its ability to discriminate against fluorescence originating from regions outside the focal plane. The contribution of fluorescence from each axial plane can be computed from the PSF and is shown in Figure 4 (see color insert). Assuming negligible attenuation, one can see that the total fluorescence generated is constant for each axial plane in one-photon microscopy. In contrast, the total two-photon fluorescence falls off rapidly away from the focal plane, demonstrating that most of the fluorescence generated is limited to the focal region.

This localized excitation volume results in greatly improved axial depth discrimination and improvement in image contrast, compared with conventional microscopy. This localization has other important consequences. First, reducing the region of photointeraction significantly decreases total specimen photobleaching

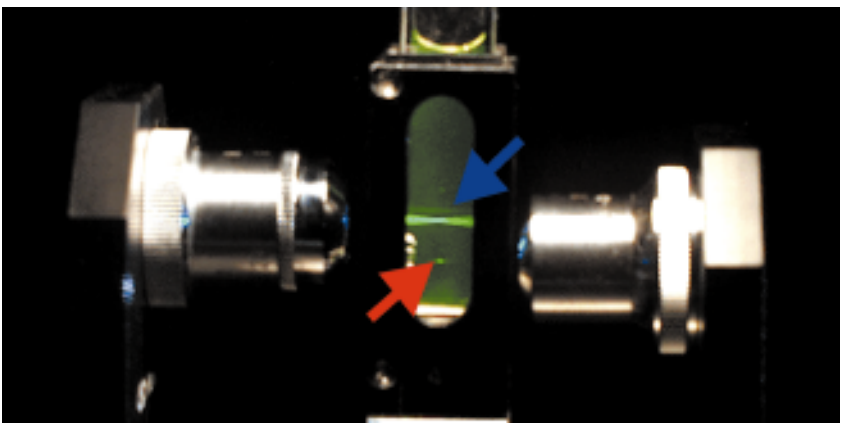

Figure 2 A comparison of one- and two-photon excitation profiles. Fluorescein solution is excited by one-photon excitation (*blue arrow*) via a 0.1-numerical-aperture objective; fluorescence excitation is observed throughout the path of the laser beam. For two-photon excitation by using a second objective with the same numerical aperture (*red arrow*), fluorescence excitation occurs only within a 3-D localized spot.

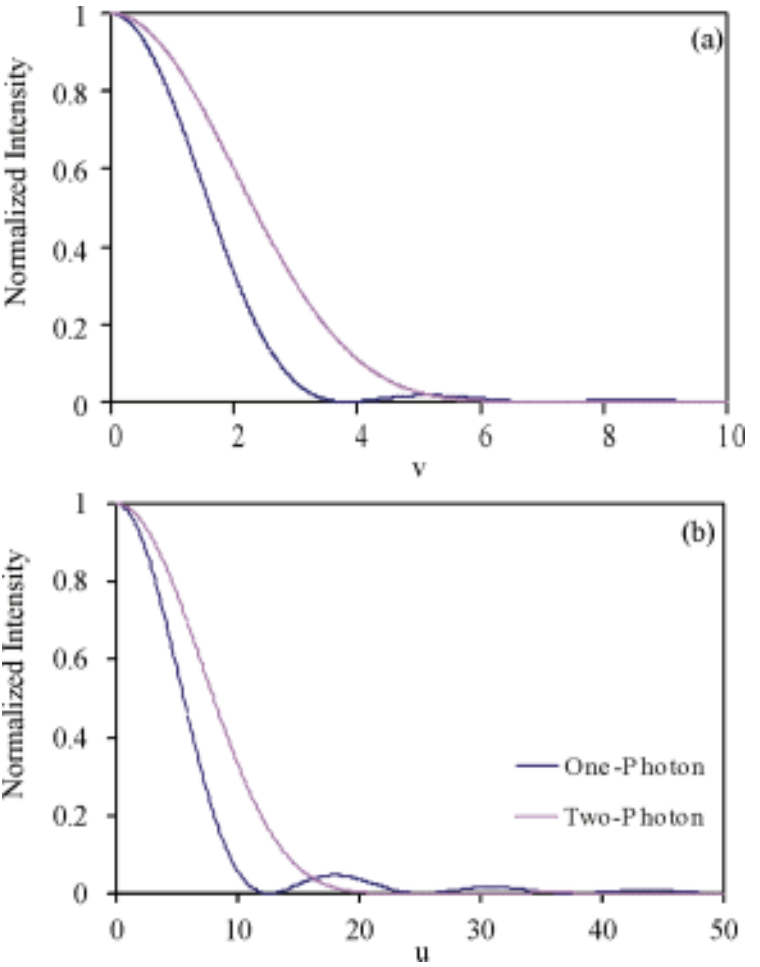

Figure 3 A comparison of the one- and two-photon point spread functions in the (*a*) radial and (*b*) axial directions. In these figures, *v* and *u* are normalized optical coordinates along radial and axial directions as defined in the main text.

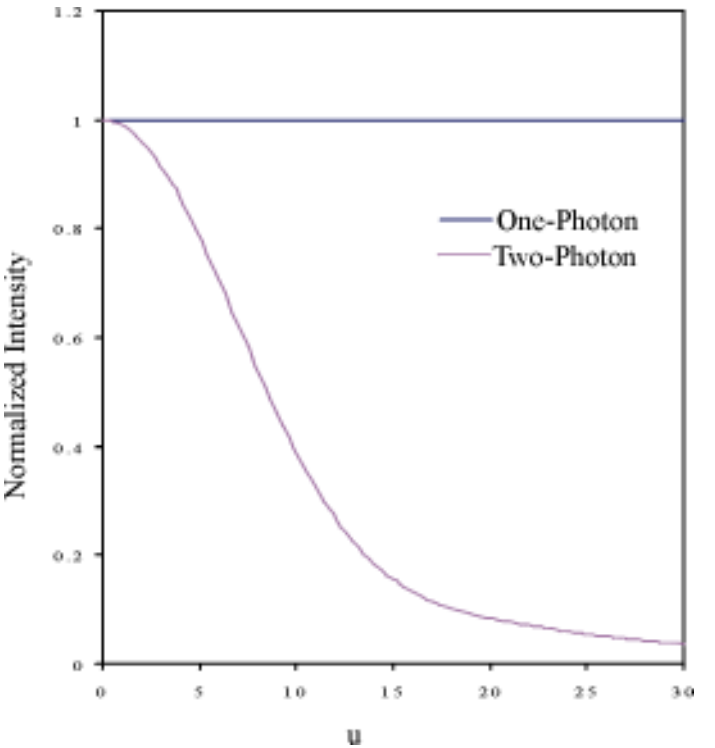

Figure 4 Total fluorescence generated at a given z-plane is calculated. This quantity is plotted as a function of its distance from the focal plane. In the one-photon case, equal fluorescence intensity is observed in all planes and there is no depth discrimination. In the two-photon case, the integrated intensity decreases rapidly away from the focal plane.

and photodamage. Second, photoinitiated chemical reaction can be locally triggered in 3-D–resolved volumes.

Reduced Attenuation in Biological Specimens Another major advantage of TPE is its ability to image thick biological specimens, owing to the reduced scattering and absorption of near IR light (relative to UV and visible wavelengths) in biological samples. In Rayleigh scattering, the scatterer is much smaller than the wavelength of light, and the scattering cross-section is inversely proportional to the fourth power of wavelength. When the equivalent wavelengths are used in OPE and TPE, a scattering event in a two-photon transition is over an order of magnitude less likely to occur than its one-photon counterpart. This results in deeper penetration of the excitation source into scattering samples. Rayleigh scattering is only an approximation of how light propagates in tissues, but the general inverse relationship between scattering and excitation wavelength remains valid. Most tissue also has reduced absorption in the near IR, thus TPE can effectively exploit the tissue "optical window" at 700–1000 nm. Tissue absorbance in this window is orders of magnitude less than the absorption in the UV or blue-green region. The deep penetration depth of TPM is a result of both reduced scattering and reduced absorption.

High Signal-to-Background Ratio Fluorescence Detection In standard one-photon microscopy, the excitation wavelength is spectrally close to the fluorescence emission band. To eliminate the leak-through of the excitation light into the detection channel, the barrier filter often cuts off a part of the emission band. The result is a reduction in microscope sensitivity. For TPE, the excitation wavelength is much farther removed from the emission band, and highly efficient filters can be applied to eliminate the excitation with a minimal attenuation of the signal.

TWO-PHOTON MICROSCOPY INSTRUMENTATION

Two-photon microscopes are commercially available; however, one can also be constructed from components (29) or by modifying an existing confocal microscope (1, 30). The basic designs of these systems are very similar, and the critical components are shown in Figure 5 (see color insert). A typical two-photon microscope features three basic components: an excitation light source, a high-throughput scanning fluorescence microscope, and a high-sensitivity detection system.

Two-Photon Laser Sources

Because two-photon absorption is a second-order process with a small cross-section on the order of 10^{-50} cm^4 s (defined as 1 GM in honor of Göppert-Mayer), high-photon flux needs to be delivered to the sample to generate efficient

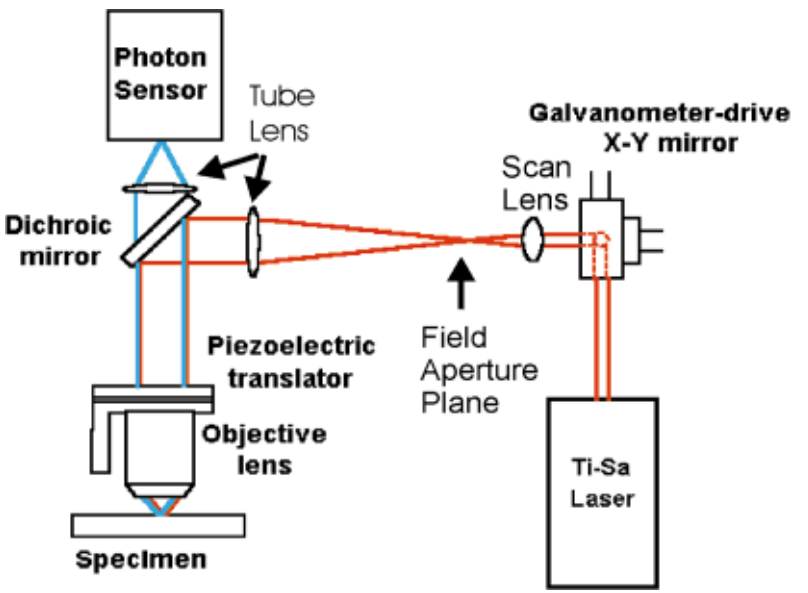

Figure 5 Schematic of a typical two-photon microscope. The excitation light path is marked in *red* and the emission light path is marked in *blue*.

absorption. This is typically achieved using ultrashort pulsed laser excitation. It has been pointed out that n_a, the number of photons absorbed per fluorophore per pulse, is given by

$$n_a \approx \frac{p_0^2 \delta}{\tau_p f_p^2} \left(\frac{(NA)^2}{2\overline{h}c\lambda} \right)^2 \quad (3)$$

where τ_p is the pulse duration, δ is the fluorophore's two-photon absorption at wavelength λ, p_0 is the average laser intensity, f_p is the laser's repetition rate, *NA* is the numerical aperture of the focusing objective, and $\overline{h}$ and c are Planck's constant and the speed of light, respectively (1). Equation 3 shows that, for the same average laser power and repetition frequency, the excitation probability is increased by increasing the NA of the focusing lens and by reducing the pulse width of the laser. Increasing NA corresponds to spatially confining the excitation power to a smaller focal volume.

Femtosecond, picosecond, and continuous-wave (cw) laser sources have been used for TPM. Currently, the most commonly used laser source for multiphoton microscopy is femtosecond titanium-sapphire (Ti-Sapphire) systems. These pulsed femtosecond systems are capable of generating a 100-fs pulse train at repetition rates of ~80 MHz. The tuning range of Ti-Sapphire systems extends from 700 to 1000 nm. Other commonly used femtosecond sources are Cr-LiSAF and pulse-compressed Nd-YLF lasers (31). From Equation 3, it is clear that TPE can also be generated by using picosecond light sources, although at a lower excitation efficiency. Commonly available picosecond systems include mode-locked Nd-YAG (~100 ps), picosecond Ti-Sapphire lasers, and pulsed-dye lasers (~1 ps). TPE with cw lasers has also been demonstrated. Compared with a standard femtosecond light source, a cw light source requires an ~200-fold increase in average power to achieve the same excitation rate. This has been accomplished using cw sources such as ArKr laser and Nd-YAG laser (32). The main advantage in using cw laser sources is the significant reduction in system cost.

Scanning Fluorescence Microscopy Optics

In a typical two-photon microscope, images are generated by raster scanning the *x-y* mirrors of a galvanometer-driven scanner. After appropriate beam power control and pulse width compensation, the excitation light enters the microscope via a modified epiluminescence light path. The scan lens is positioned such that the *x-y* scanner is at its eye point while the field aperture plane is at its focal point. For infinity-corrected objectives, a tube lens is positioned to recollimate the excitation light. The scan lens and the tube lens function together as a beam expander that overfills the back aperture of the objective lens. A dichroic mirror reflects the excitation light to the objective. The dichroic mirrors are short-pass filters, which maximize reflection in the IR and transmission in the blue-green region of the spectrum. Typically, high-numerical-aperture objectives are used to maximize excitation efficiency. The *x-y* galvanometer-driven scanners provide lateral

focal-point positioning. An objective positioner translates the focal point axially and allows 3-D raster scanning.

Fluorescence Detection System

The fluorescence emission is collected by the imaging objective and transmitted through the dichroic mirror along the emission path. An additional barrier filter is needed to further attenuate the scattered excitation light because of the high excitation intensity used. The fluorescence signal is directed to the detector system. Photodetectors that have been used in two-photon microscope systems include photomultiplier tubes (PMTs), avalanche photodiodes, and charge-coupled-device (CCD) cameras. PMTs are the most common implementation because they are robust and low cost, have large active areas, and have relatively good sensitivity.

A major advantage of TPM is that, unlike confocal microscopy, emission pinholes and descanning optics are not necessary to achieve axial depth discrimination. TPE is already localized to the focal volume, and there is no appreciable off-focal fluorescence to reject. The addition of a pinhole can enhance resolution but at a cost of signal loss (33, 34). An important consideration in designing the detection pathway is whether to implement a de-scan lens in the emission path. If the scanned region in the object plane is d, then the de-scan lens is not necessary if the detector area is larger than a characteristic area given by $d \times M$, where M is the overall magnification of the detection path (35). However, for nonuniform detectors, as some PMTs are, it may be desirable to implement descanning optics to prevent detection efficiency variation when the fluorescence emission is incident on different positions of the photocathode surface.

FLUORESCENT PROBES USED IN TWO-PHOTON MICROSCOPY

It is important to examine the nonlinear absorption characteristics of fluorescent molecules. In general, most chromophores can be excited in two-photon mode at twice their one-photon absorption maximum. However, because one- and two-photon absorption processes have different quantum mechanical selection rules, a fluorophore's TPE spectrum scaled to half the wavelength is not necessarily equivalent to its OPE spectrum. Spectroscopic properties of fluorophores under nonlinear excitation need to be better quantified to optimize their use in TPM. Below, we discuss the two-photon absorption properties of some typical extrinsic and intrinsic fluorophores.

Extrinsic and Endogenous Two-Photon Fluorophores

The spectroscopic study of rhodamine under TPE was one of the earliest efforts in this area (36). With the advent of TPM, spectral characterization of fluorophores

TABLE 1 Two-photon cross-sections of some common fluorophores[a]

Fluorophores[b]	Excitation wavelength (nm)	$\eta_2\delta$ (10^{-50} cm^4 s/photon)	δ (10^{-50} cm^4 s/photon)
Extrinsic fluorophores			
Rhodamine B	840		210 (±55)
Fluorescein (pH 11)	782		38 (±9.7)
Fura-2 (free)	700	11	
Fura-2 (with Ca^{2+})	700	12	
Indo-1 (free)	700	4.5 (±1.3)	12 (±4)
Indo-1 (high Ca)	700	1.2 (±0.4)	2.1 (±0.6)
Bis-MSB	691	6.0 (±1.8)	6.3 (±1.8)
Dansyl	700	1	
Dansyl hydrazine	700	0.72 (±0.2)	
$DiIC_{18}$	700	95 (±28)	
Coumarin-307	776	19 (±5.5)	
Cascade blue	750	2.1 (±0.6)	
Lucifer yellow	860	0.95 (±0.3)	
DAPI	700	0.16 (±0.05)	
BODIPY	920	17 (±4.9)	
Intrinsic fluorophores			
GFP wild type	∼800		∼6
GFP S65T	∼960		∼7
NADH	∼700		∼0.02
FMN	∼700		∼0.8
Phycoerythrin	1064		322 (±110)

[a]η_2, Fluorescence quantum efficiency under two-photon excitation (35, 42, 161).

[b]Abbreviations: Bis-MSB, p-bis(o-methylstyryl) benzene; $DiIC_{18}$, octadecyl indocarbo cyanine; DAPI, 4′,6-diamidino-2-phenylindole; BODIPY, 4,4-difluoro-1,3,5,7,8-pentamethyl-4-bora-3a,4a-diazaindacene-2,6-disulfonic acid disodium salt; GFP, green fluorescent protein; NADH, reduced nicotinamide-adenine dinucleotide; FMN, flavin mononucleotide.

under nonlinear excitation took on a new urgency (37, 38). Extrinsic fluorophores are organic molecules that are designed to label biological structures and to measure biochemical functions. Recently, absorption spectra of many extrinsic fluorophores have been determined. A summary of absorption properties of these extrinsic fluorophores is presented in Table 1.

In addition to extrinsic fluorophores, biological systems often possess endogenous fluorescent molecules that can be imaged, revealing important sample characteristics without the need for labeling. Two-photon–induced fluorescence from tryptophan and tyrosine in proteins has been investigated (39–41). More recently,

the absorption cross-section of phycoerythrin has been measured and shown to be much greater than that of rhodamine 6G at the excitation wavelength of 1064 nm (42). Multiphoton-induced fluorescence of the neurotransmitter serotonin has also been demonstrated (43). The exciting development of green fluorescent protein (GFP) introduces a convenient fluorescent marker for monitoring gene expression in cells and tissues (44). Two-photon imaging parameters of the GFPs have been optimized (45, 46). Nicotinamides [NAD(P)Hs] represent another intrinsic fluorophore that can be excited by using a two-photon microscope (41). NAD(P)H levels in cells are related to their metabolic rates (47), and NAD(P)H fluorescence has been used to monitor redox state in cornea (48) and skin (49). The two-photon spectroscopic characteristics of these endogenous probes are also listed in Table 1.

Recent Efforts in Two-Photon Probe Development

One recent development in two-photon probe utilization has been in identifying drug molecules that are excitable by two-photon light sources. The ability to monitor the drug distribution in a native environment allows a better assessment of drug delivery efficiency and can be important for developing therapeutic strategies (50). However, monitoring fluorescent drugs under physiological conditions with OPE can be difficult because of short image penetration depth and high background fluorescence contribution from other naturally occurring fluorescent compounds (51). Therefore, the identification of two-photon excitable drugs has important clinical and pharmaceutical consequences. In this area, the anticancer drug topotecan has been identified as a good two-photon probe with a two-photon absorption cross-section of >20 GM at 840-nm excitation. Under physiological conditions, two-photon–induced fluorescence from topotecan has been detected in plasma and in whole blood down to respective concentrations of 0.05 μM and 1 μM (51). In the foreseeable future, it is likely that further efforts in identifying two-photon–excitable pharmaceutical agents for implementation in clinical settings will be made.

Another important area is the development of extrinsic fluorophores with optimal two-photon absorption properties. The fluorophores listed in Table 1 have all been conventional one-photon excitable probes. Because OPE and TPE obey different selection rules, one should not expect these probes necessarily to have optimized properties for TPE. Recent searches for molecules with high two-photon absorption cross-sections have led to discovery of molecules with two-photon cross-sections of >1000 GM (52). Optimizing two-photon absorption properties in fluorophores has two important consequences. The development of efficient fluorophores can reduce the excitation laser intensity required for imaging, and thus reduce specimen photodamage. Alternatively, with high two-photon cross-sections, significant excitation can be achieved with the more economical cw lasers, thus reducing the cost of two-photon systems that typically use femtosecond Ti-Sapphire lasers.

PHYSIOLOGICAL EFFECTS OF NEAR-IR MICROBEAM ILLUMINATION

TPE reduces specimen photodamage by localizing the excitation region to within an 1-fl volume. Photodamage is also decreased by use of near-IR excitation rather than UV and visible radiation. Decreasing the photochemical-interaction volume results in a dramatic increase in biological-specimen viability. The noninvasive nature of two-photon imaging can be best appreciated in a number of embryology studies. Previous work on long-term monitoring of *Caenorhabditis elegans* and hamster embryos, using confocal microscopy, has failed because of photodamage-induced developmental arrest. However, recent TPM studies indicate that the embryos of these organisms can be imaged repeatedly over the course of hours without observable damage (53–55). It is more important that the hamster embryo was reimplanted after the imaging experiments and eventually developed into a normal, healthy, adult animal.

At the focal volume at which photochemical interactions occur, TPM can still cause considerable photodamage. Three major mechanisms of two-photon photodamage have been recognized. (*a*) Oxidative photodamage can be caused by two- or higher photon excitation of endogenous and exogenous fluorophores with a photodamage pathway similar to that of UV irradiation. These fluorophores act as photosensitizers in photooxidative processes (56, 57). Photoactivation of these fluorophores results in the formation of reactive oxygen species that trigger the subsequent biochemical damage cascade in cells. Current studies have found that the degree of photodamage follows a quadratic dependence on excitation power, indicating that the two-photon process is the primary damage mechanism (58–62). Experiments have also been performed to measure the effect of laser pulse width on cell viability. Results indicate that the degree of photodamage is proportional to two-photon excited fluorescence generation, and is independent of pulse width. Hence, using shorter wavelength for more efficient TPE also produces greater photodamage. An important consequence is that both femtosecond and picosecond light sources are equally effective for two-photon imaging in the absence of an IR one-photon absorber (59, 61). Flavin-containing oxidases have been identified as one of the primary endogenous targets for photodamage (62). (*b*) One- and two-photon absorption of the high-power IR radiation can also produce thermal damage. The thermal effect resulting from two-photon water absorption has been estimated to be on the order of 1 mK for typical excitation power and has been shown to be insignificant (3, 63). However, in the presence of a strong IR absorber such as melanin (64, 65), there can be appreciable heating caused by one-photon absorption. Thermal damages have been observed in the basal layer of human skin in the presence of high average-excitation power (66). (*c*) Photodamage may also be caused by mechanisms resulting from the high peak power of the femtosecond laser pulses. There are indications that dielectric breakdown occasionally occurs (58). However, further studies are required to confirm and better understand these effects.

MOLECULAR-LEVEL APPLICATIONS OF TWO-PHOTON MICROSCOPY

In recent years, a number of technological advances in light sources, detectors, and optics have led to tremendously improved sensitivity in fluorescence methods. Single-molecule sensitivity is now routinely achieved (67–70). Although most of the single-molecule work has used OPE, two-photon methods can offer improvement in the signal-to-background ratio (SBR), owing to excitation volume localization and the wide spectral separation of the emission, excitation, and Raman bands.

It should be noted that, although ultrasensitive applications of two-photon fluorescence require careful optimization of instrumentation and experimental setups, they are not fundamentally different from two-photon fluorescence instrumentation discussed previously in this review. The following discussion of single-molecule applications of two-photon fluorescence has been divided into three parts: fluorescence burst detection of single molecules, single-molecule imaging, and fluorescence correlation spectroscopy (FCS).

Single-Molecule Detection in Solution

The first demonstration of single-molecule detection by TPE in solution was presented by Mertz et al (71), using rhodamine B molecules in water. They observed photon bursts from single molecules diffusing through the two-photon volume, with an average SBR of $\sim$10. A number of other reports have since demonstrated efficient fluorescence burst detection of single molecules by TPE in free solution (72, 73), in flow cells (74–76), and in low-temperature solids (77, 78). As anticipated, a common finding among most of these reports is the high SBR, largely caused by the very low background levels associated with TPE. A quantitative study of the two-photon background, including contributions from two-photon hyper-Rayleigh and hyper-Raman scattering of water, has shown reduced background levels for TPE vs OPE (79). Care must be taken in determining TPE illumination conditions, because too much input power can lead to continuum generation in the solvent, and thus greatly increased background levels (73).

Although the SBR has generally been favorable with TPE, the absolute count rates per molecule are not always comparable with OPE detection (71, 73, 80–82). The reduced magnitude of fluorescence yield is hypothesized to arise from long-lived, more highly excited states reached by TPE, increased photobleaching, intersystem crossing, or perhaps some other saturation or multiphoton phenomena. The mechanism is sample dependent, and there are counter examples in which the TPE fluorescence intensity is comparable with (enhanced green-fluorescence protein) or exceeds (7-amino-A-methylcoumarin) the OPE fluorescence level, at least under certain illumination conditions (73, 83). The photophysics of a given molecule of interest is thus important in determining the relative advantages of one- and two-photon fluorescence detection. Newly designed chromophores with high two-photon cross-sections may enhance the advantages of TPE in single-molecule applications (52, 84).

Imaging Single Molecules with Two-Photon Excitation

Spatially resolved applications of ultrasensitive two-photon fluorescence have also shown promising results. Sanchez and coworkers first demonstrated two-photon imaging (far-field) of single rhodamine B molecules immobilized on glass surfaces with an SBR of 30 (80). In addition, emission spectra were acquired for individual molecules by using a cooled CCD and a spectrograph. Discrete photobleaching of individual fluorescence peaks, as well as polarized emission, served as evidence for true single-molecule detection. It is interesting that this group found that TPE leads to faster photobleaching of single rhodamine B molecules than OPE, by a factor of $\sim$2. This number is expected to be sample dependent. A report by Bopp et al, also using rhodamine B, demonstrates the ability to determine molecular orientation, as well as to measure laser pulse parameters at the sample by TPE fluorescence (85). Their results also showed reduced fluorescence emission from rhodamine B for TPE vs OPE. An interesting variation of TPE imaging methods uses two-photon "wide-field" illumination ($\sim$5-μm-diameter spot); the larger spot size is achieved by underfilling the objective lens. This approach allowed Sonnleitner et al to not only observe single molecules, but track them within the spot over time, measuring diffusion of single labeled lipid molecules (86). The authors plan to test this approach for tracking single molecules on live cell membranes.

Imaging applications of TPE have also been extended to the near-field, using uncoated fiber tips (81, 87). The study by Kirsch et al makes use of cw TPE. These applications have the exciting potential of ultraresolved imaging with high SBRs and improved *z*-resolution as compared with one-photon near-field imaging. To fully realize these advantages requires selection of fluorescent probes that are reasonably stable with TPE, because increased bleaching (as seen with rhodamine probes) would otherwise detract from the TPE advantages.

Finally, an apertureless variation of near-field imaging was recently introduced with the promise of extremely highly resolved imaging not limited by a minimum aperture size (88). An exciting direction in this field is the use of enhanced radiation (from electromagnetic interaction of the tip and the optical field) localized at the tip end to improve resolution and contrast. The quadratic dependence of TPE on excitation intensity makes it ideal to exploit these locally enhanced fields (89, 90). The first experimental realization of this approach demonstrated extremely high-resolution images ($\sim$20 nm) of photosynthetic membrane fragments and *J*-aggregates of pseudoisocyanine dye (91). Fluorescence quenching by the near-field probe is a problem for this method, which, nonetheless, has very exciting possibilities.

Fluorescence Correlation Spectroscopy

FCS, first introduced by Magde et al (92) and Thompson (93), is proving to be a powerful method for studying a large variety of experimental systems. Applications include measurement of diffusion, chemical reactions, molecular interactions, number concentration, hydrodynamic flow, and photophysical parameters

such as triplet state lifetimes. FCS experiments are performed by recording spontaneous equilibrium fluctuations in fluorescence intensity (i.e. fluorescence bursts) from a small (<1-fl) open volume. Information about various experimental parameters is extracted through temporal analysis of these fluctuations by calculating the autocorrelation (or cross correlation) of the fluorescence signal, defined as

$$G(\tau) = \frac{\langle \delta F(t) \times \delta F(t+\tau) \rangle}{\langle F(t) \rangle^2} \tag{4}$$

Here $F(t)$ is the time-dependent fluorescence signal, $\delta F(t)$ is the time-dependent deviation from the average fluorescence intensity, and the angle brackets represent the time average. Because this review is focused on TPM, we here cover only two-photon FCS measurements, and the reader is referred to the above references for a more general discussion and review of the FCS literature.

TPE was first applied in FCS measurements by Berland et al. The optical sectioning of TPE was introduced as an alternative to confocal detection for FCS in 3-D systems (94). This report demonstrated the capability to measure translational diffusion coefficients of small (7- and 15-nm radius) fluorescent latex beads in solution and, for the first time using FCS, in the cytoplasm of live cells (Figure 6). The low background levels associated with TPE and reduced autofluorescence achieved by using 960-nm excitation were of critical importance for the cellular measurements. A subsequent report by these authors introduced the capability to measure molecular concentration and thus detect protein association/dissociation reactions and kinetics in solution (95). As mentioned above, FCS can also be a powerful tool in studying the photophysical characteristics of fluorescence probes,

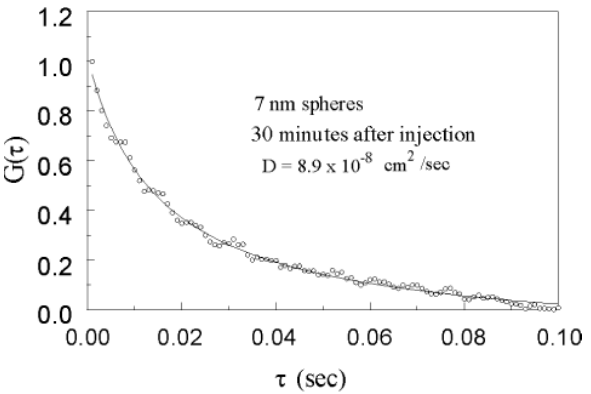

Figure 6 Result of a fluorescence correlation spectroscopic measurement of the diffusion coefficient of 7-nm-radius latex spheres in the cytoplasm of CRL 1503 mouse embryonic fibroblast cells. The data are acquired 30 min after microinjection. The diffusion rate (8×10^{-8} cm^2/s) is found to be ~fivefold slower than in water (3×10^{-7} cm^2/s). This figure is adapted from 94.

and FCS analysis provided an important tool in deciphering the fluorescence properties of the UV probe Coumarin-120 with both OPE and TPE (73). In addition to the general interest of these findings, the results from this type of analysis provide valuable information, which is useful for experimental design, particularly for two-photon imaging applications in which optimal experimental conditions are not known a priori.

The main motivation for using two-photon FCS in a given experiment, rather than one-photon confocal FCS, is to exploit the same features (discussed elsewhere in this review) that make TPE advantageous in other experiments. A very thorough comparison of OPE and TPE FCS applications can be found in a recent publication by Schwille et al (83). This excellent paper demonstrates that FCS measurements of diffusion can be performed at the single-molecule level in live cells, with similar results from both one- and two-photon FCS. Illumination and detection conditions were carefully chosen, such that the fluorescence yield was similar for both OPE and TPE. Their results resolve diffusion of rhodamines in the cytoplasm and membranes, and of Cy-3 (Amersham Pharmacia Biotech, Uppsala, Sweden)-labeled immunoglobulin E receptors in the membrane of several different cell types. The diffusion data show interesting complexity, suggesting anomalous diffusion or at least multicomponent diffusion. Whereas FCS was possible in cells using OPE, a number of TPE advantages were confirmed. First, TPE FCS measurements were possible in regions in which OPE FCS was not, such as within plant cells with highly scattering cell walls. A second major advantage was the reduced photobleaching of molecules outside the observation volume (as compared with OPE confocal). This can be exceedingly important when there are small numbers of fluorescent molecules in a cell to begin with. Third, TPE provided superior axial resolution and the ability to confine the FCS signal to a given cell region. Finally, the SBR can also be higher for TPE, depending on probes and cell types. One distinct disadvantage is that, for illumination conditions yielding comparable fluorescence intensity, TPE power levels are substantially closer to the biological damage threshold.

Photon-Counting Histogram

The photon-counting histogram (PCH) has recently been proposed as an alternative approach to FCS for analyzing photon burst data, to accurately measure sample concentrations and detect molecular interactions (96, 97). Rather than analyzing the temporal behavior of fluorescence fluctuations, the PCH analyzes the fluctuation amplitude distributions. Chen et al have demonstrated that PCH analysis can describe fluorescence fluctuation data as a super-Poissonian distribution with great precision (97). Fluctuation data were obtained from TPE measurements of several fluorescent dyes in solution. This type of analysis is expected to be quite powerful for measuring molecular concentration and detecting and quantifying molecular interactions, as was already demonstrated for two-component systems (96).

CELLULAR-LEVEL APPLICATIONS OF TWO-PHOTON MICROSCOPY

The ability to simultaneously monitor cellular biochemical activity and structure at the subcellular level is vital to understand many important processes. The need for functional imaging dictates the use of minimally invasive technology such as TPM. The ability of TPE to initiate photochemial reaction in a subfemtoliter volume further opens up new windows of opportunities for 3-D, localized uncaging and photobleaching experiments.

Two-Photon In Vivo Cellular Imaging—Minimizing Photodamage and Bleaching

Although higher-resolution methods such as electron microscopy can produce images with finer details, optical microscopy is unique because it reveals dynamic processes such as signaling, intracellular transport, and cell migration. Some cellular processes have been successfully studied with white light video microscopy (98). However, many functional studies require fluorescence. Fluorescence imaging of live cells is difficult, especially when 3-D information is required. Before the invention of TPM, fluorescence confocal microscopy was the only option. The use of high-intensity UV or blue-green radiation in the confocal system results in significant photodamage and compromises the validity of the research.

This difficulty has been alleviated with the introduction of two-photon imaging. TPM enables a number of difficult studies in which sensitive specimens may be damaged under UV excitation. The study of cellular calcium signaling is one of these areas where TPE can contribute (99). The feasibility of using indicators, such as Indo I (100) and Calcium Green (29) (Molecular Probes, Eugene, OR), in two-photon microscopes for the quantification of cellular calcium level has been demonstrated. TPM has been used successfully in calcium-signaling studies such as the effect of calcium signals in keratocyte migration (101) and the mapping of the calcium channel in hair cells (102). Two-photon imaging has also been applied in systems in which the available fluorescent indicators are not very photostable. An example is the measurement of membrane fluidity in cells and vesicles with the generalized polarization probe Laurdan, which is easily photobleached (103–105).

Multiphoton Imaging of Far-UV Fluorophores

Another interesting application of multiphoton excitation is the imaging of serotonin distribution in cells (106). Serotonin is an important neural transmitter. The far-UV ($\sim$240-nm) fluorescence excitation of serotonin makes optical microscopic studies of serotonin biology difficult. Using a conventional microscope, this spectral region is virtually inaccessible. Maiti et al (106) realized that multiphoton excitation can be used to image this class of chromophores. Serotonin was excited in the near IR by three-photon absorption, and they have demonstrated that the

distribution of serotonin in intracellular granules can be mapped. Equally important is the subsequent discovery by Shear et al (43) that serotonin may be further excited by a six-photon process in which the molecule is converted by the absorption of four photons to a two-photon–excitable by-product. Serotonin distribution can then be imaged based on the blue-green fluorescence of this by-product (43). The two basic principles described here are important. First, multiphoton excitation can be used to access new far-UV chromophores. Second, multiphoton chemical processes may be used to create new fluorophores based on endogenous cellular molecules.

Two-Photon Multiple Color Imaging

The possibility of using TPM to simultaneously excite different color fluorophores for multiple label imaging has been explored (29, 107) (Figure 7; see color insert). Xu et al imaged rat basophilic leukemia cells simultaneously labeled with pyrene lysophosphatidylcholine, a UV-emitting plasma membrane probe; DAPI, a blue-emitting nucleic probe; Bodipy sphingomyelin, a green-emitting Golgi label; and rhodamine 123, a red-emitting mitochondria probe. This study demonstrates the simultaneous imaging of four cellular structural components and the potential for studies in which the interaction of various cellular organelles can be monitored over time in 3-D.

Three-Dimensional Localized Uncaging of Signaling Molecules

An important property of TPM is its ability to initiate localized chemical reactions such as the uncaging of signaling molecules. Denk led the development of this novel technique by mapping the distribution of nicotin acetylcholine receptors in a muscle cell line (BC3H1) (108). The membrane potential of a chosen cell was monitored by the whole-cell patch clamp technique. Caged carbamoylcholine was placed in the medium. Upon two-photon uncaging, a 3-D localized burst of carbamoylcholine was released at the focal point of the laser light. The whole-cell current measured by the patch clamp is a function of the relative spatial distance between the carbamoylcholine burst and the proximal acetylocholine receptors. In the presence of many close-by receptors, a larger current will be observed and vice versa. By scanning the uncaging beam throughout the cell volume, the receptor distribution can be determined. Similar techniques have been subsequently applied to map glutamate receptors on hippocampal pyramidal neurons (109).

In addition to receptor mapping, localized uncaging is also valuable for the study of intracellular-signaling pathways. The ability to generate active signaling molecules localized in 3-D with submicrometer resolution allows investigators to monitor intracellular signal propagation. Localized uncaging of fluorescein has been demonstrated by Denk and coworkers (1). However, the uncaging of more important cellular messengers, such as calcium, has been difficult because of the

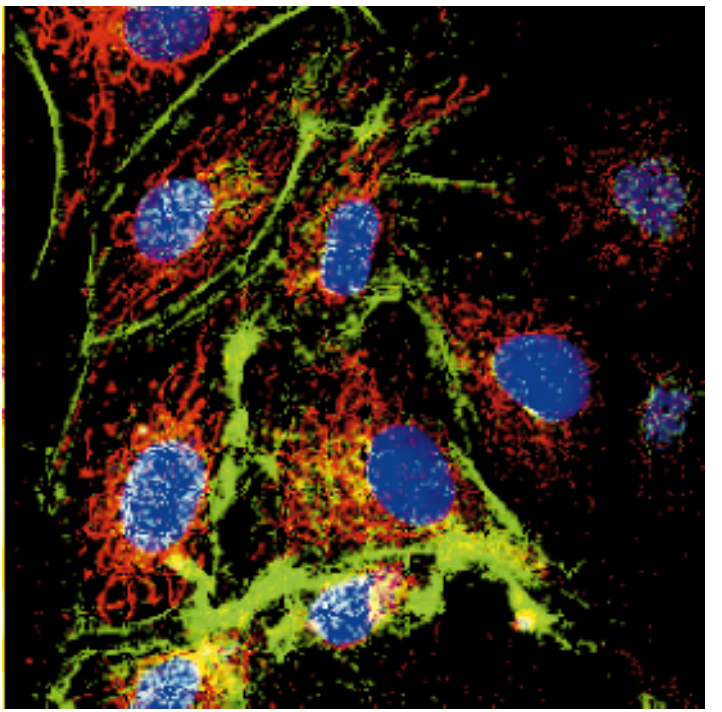

Figure 7 Two-photon multiple color imaging of bovine pulmonary artery endothelial cells labeled with DAPI (nucleus), BODIPYO-FL phallacidin (actin), and MitoTrackero Red CMXRos (mitochondria) (Molecular Probes, Eugene, OR). All three probes were excited at 780 nm, and images were acquired by three independent detection channels.

lack of an efficient two-photon photolabile cage. This situation is improving as new cage groups targeted for two-photon applications are being developed (110). This new technology has been used in a number of pilot studies (111–116).

Two-photon photobleaching recovery is a similar technique that can be applied to measure intracellular transport, viscosity, and diffusion (117). Similar to conventional photobleaching-recovery studies, molecules labeled with fluorophores of interest can be photobleached within a 3-D localized volume. The recovery of loss fluorescence is correlated with fresh molecules diffusing back into the excitation volume and provides information on the intracellular environment.

TISSUE LEVEL APPLICATIONS OF TWO-PHOTON MICROSCOPY

A recent comparison study has convincingly demonstrated that TPM is a superior method in the imaging of thick, highly scattering specimens (33).

Applying Two-Photon Microscopy to Study Tissue Physiology

The potential of applying TPM to study tissue physiology has been recognized since its inception (1). Two-photon tissue imaging has been successfully applied to study the physiology of many tissue types, including the corneal structure of rabbit eyes (48, 66), the light-induced calcium signals in salamander retina (118), the human and mouse dermal and subcutaneous structures (49, 119, 120) (Figure 8; see color insert), the toxin effect on human intestinal mucosa (121), and the metabolic processes of pancreatic islets (122, 123). Today, TPM is particularly widely used in two areas—neurobiology (124) and embryology. In neurobiology studies, TPM has been applied to study the neuron structure and function in intact brain slices (125), the role of calcium signaling in dendritic spine function (126–134), neuronal plasticity and the associating cellular morphological changes (135), and hemodynamics in rat neocortex (136). In embryology studies, two-photon imaging has been used to examine calcium passage during sperm-egg fusion (137), the origin of bilateral axis in sea urchin embryos (138), cell fusion events in *C. elegans* hypodermis (53, 54), and hamster embryo development (55). It is expected that two-photon imaging will be applied to an increasing number of tissue systems as better commercial instruments become available.

It is important to examine the technological limitations of applying two-photon imaging in tissues. (*a*) It should be recognized that the imaging depth of different specimens could be drastically different. For example, in the cornea of the eye, a unique optically transparent organ, an autofluorescence image can be obtained from depths beyond a millimeter, whereas, inside a highly scattering specimen such as human skin, the contrast of autofluorescence images is significantly degraded at $\sim$200–300 μm. The maximum imaging depth depends on the scatteering

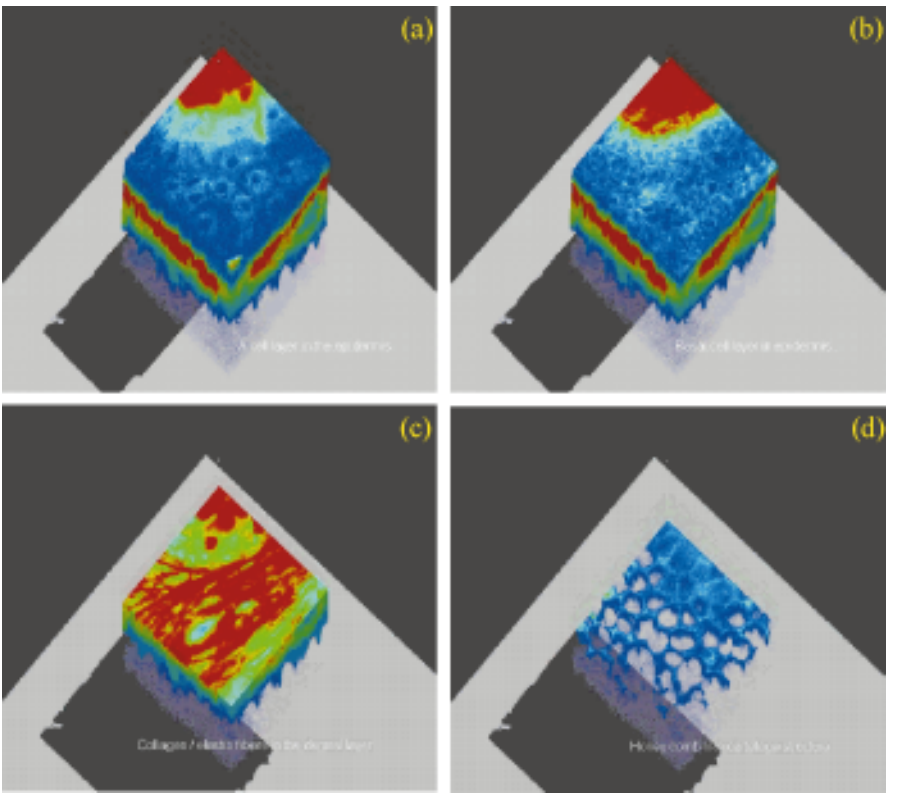

Figure 8 Three-dimensional reconstructed two-photon images of dermal and subcutaneous structures in a mouse ear tissue specimen. The four panes show distinct structural layers: (*a*) epidermal keratinocytes, (*b*) basal cells, (*c*) collagen/elastin fibers, and (*d*) cartilage structure. This figure is adapted from (120).

and absorption coefficients of the tissue, the efficiency of the fluorophore, and the throughput of the microscope optics. (*b*) The two-photon PSF is well characterized in thin specimens. In a number of tissue models, two-photon PSF degradation appears to be minimal up to a depth of 100 μm (33). However, the aberration of PSF in real tissue specimens has not been satisfactorily measured. A number of projects are now underway to better understand the physics of light propagation in turbid medium and to quantify resolution in both tissue phantoms and real tissues. (*c*) Fluorescence labeling of deep tissue structure is a major technical challenge. Common fluorescent probes are designed for labeling cultured cells. Diffusional delivery of these probes is not ideal in tissues. Probe distributions tend to vary greatly as a function of depth. Fluorophores could also be delivered by microinjection, but this method suffers from its invasive nature and its limited ability to label multiple cells. Tissue structure may also be imaged with endogenous fluorophores such as NAD(P)H and flavoproteins (47). Unfortunately, these fluorophores suffer from low quantum yield, and their fluorescence emissions in the blue-green spectral region are strongly attenuated by the tissue. Molecular biology methods allow the labeling of specific tissue structures with fluorescent probes such as GFP, but this method can be applied only to specimens with well-controlled genetic makeup. The lack of universal and effective methods for fluorescent labeling of living tissues is a major obstacle in two-photon tissue imaging.

Applying Two-Photon Excitation for Clinical Diagnosis and Treatment

A promising direction for two-photon tissue imaging is clinical diagnosis and treatment. Optical biopsy is a new paradigm in clinical diagnosis. Traditional biopsy requires the removal, fixation, and imaging of tissues. The histological procedure is invasive, and tissue biochemical information is poorly preserved during these preparation steps. Optical biopsy based on TPE has been proposed in which 3-D images of tissues will be noninvasively acquired from patients. The image stack will be subsequently subjected to pathological analysis. TPM has been successfully used to image the skin structure of human volunteers down to a depth of 150 μm (49, 139). Four distinct structural layers in the epidermis and the dermis are typically resolved (Figure 9; see color insert). The topmost layer is the stratum corneum, where the cornified cells form a protective layer. The second layer consists of epidermal keratinocytes. At the epidermal-dermal junction lies a layer of germinative basal cells. In the dermal layer, collagen/elastin fiber structures can be clearly observed. Pathological states such as atypical changes in cellular morphology or cellular hyperfoliation can often be identified. However, today, it remains unknown whether the quality of images acquired by two-photon optical biopsy is sufficient to produce pathological analysis results with accuracy comparable to that of traditional histology. If the feasibility of this technique can be demonstrated, the development of a two-photon endoscope may provide a method to biopsy other organs. Similar efforts are underway in confocal imaging (140, 141).

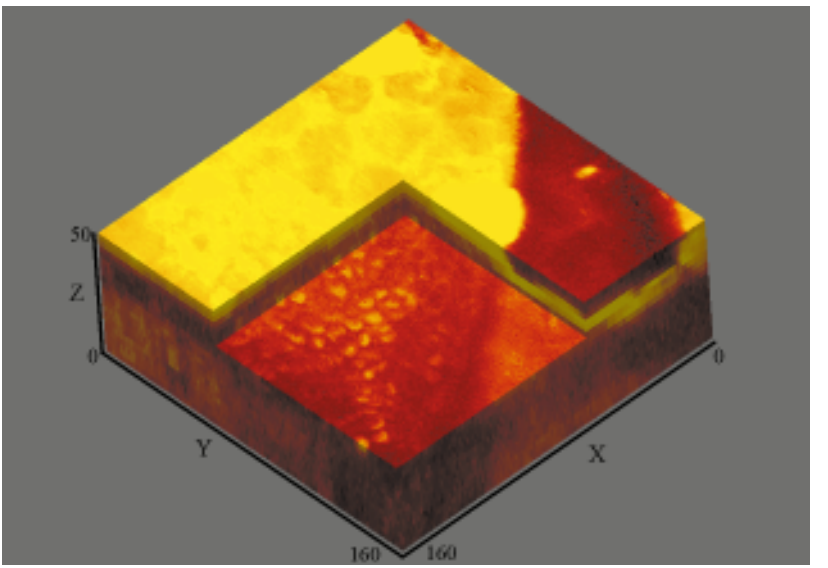

Figure 9 Three-dimensional reconstructed two-photon images of in vivo human skin. The strata corneum and the basal layers are clearly visible. The figure is adapted from (159).

In addition to diagnosis, TPE may also find applications in clinical treatment based on photodynamic therapy. Photodynamic therapy allows the destruction of specific tissue, such as a tumor, by preferentially loading the tissue with a photosensitizer. Photosensitizer-loaded tissue is subsequently destroyed by laser illumination. Unfortunately, while the photosensitizer uptake in tumorous tissue is higher, there is often non-negligible uptake in normal tissues. Peripheral damage to healthy tissues is a common occurrence. The potential of using two-photon imaging to first localize the tumor and then of applying TPE to initiate photodynamic action at the selected site is a very attractive option. Preliminary work in this area has been reported (142–144).

NEW DEVELOPMENTS IN TWO-PHOTON INSTRUMENTATION

Although the standard TPM, as described previously, functions very well as a general purpose instrument, a number of exciting new applications demand new instrumentation capabilities. This section describes the frontiers of two-photon instrumentation research and their biomedical potentials.

Two-Photon Video Rate Microscopy

A major limitation of standard two-photon microscopes is their speed, which is ~0.5 Hz, and the typical time required to obtain a high-resolution 3-D image stack is ~10 min. This is clearly unsuitable for applications such as clinical biopsy, in which efficiency is crucial. Furthermore, this slow imaging speed is also incompatible with intravital imaging of patients or animals, in which the presence of motion artifacts is a major concern. Finally, the study of many cellular processes, such as calcium signaling or neuronal communication, requires imaging with millisecond time resolution. This problem is addressed by the development of a number of video rate two-photon microscopes.

The first video rate two-photon imaging system is based on the line-scanning approach. Image acquisition time is reduced by covering the image plane with a line instead of a point (145, 146). The line focus is typically achieved by using a cylindrical element in the excitation beam path. The resulting fluorescent line image is acquired with a spatially resolved detector such as a CCD camera. The main drawback associated with line scanning is the inevitable degradation of the image PSF, especially in the axial direction. A second approach, which has been termed "multiphoton multifocal microscopy" (147, 148), is analogous to Nipkow disk-based confocal systems (149). This elegant approach is based on a custom fabricated lenslet array, in place of the scan lens, that focuses the incident laser into multiple focal spots at the field aperture plane. The lenslet lenses are arranged in patterns similar to the traditional Nipkow disk designs. Upon the rotation of the lenslet lens, the projection of the lenslet will uniformly cover the field aperture

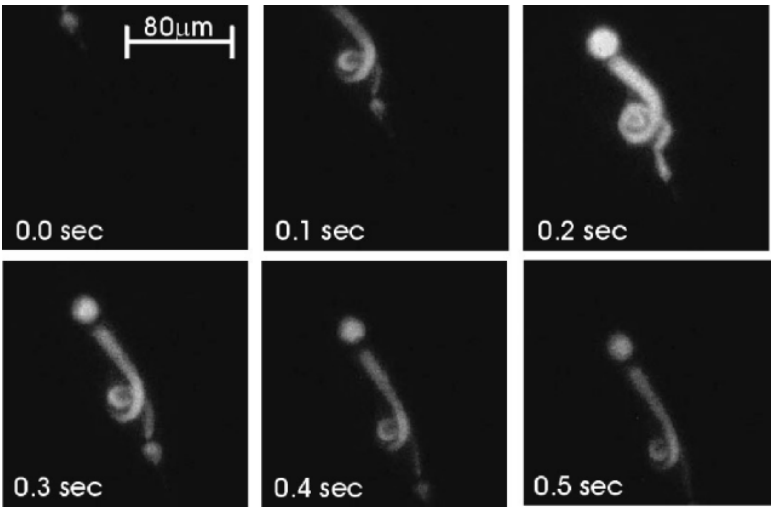

Figure 10 Video rate two-photon image of a Calcein-AM labeled protozoa, blepharisma, as it swam across the observation area at a rate of ~100 μm/s. The figure is adapted from 151.

plane. A CCD camera is used to register the spatial distribution of the resulting fluorescent spots and integrate them into a coherent image. The ability to excite multiple sample regions simultaneously reduces total data acquisition time. This technique has less resolution degradation compared with line scanning and has the added advantage of being extremely robust. A third method has been developed based on the raster scanning of a single diffraction-limited spot by using either a high-speed resonance scanner (150) or rotating polygonal mirror (151; Figure 10). In this case, a large, single-point detector, such as a photomultiplier tube or an avalanche photodiode, can be used. The spatial information is encoded by the timing design of the raster scan pattern. By replacing the CCD imager with a single pixel detector, the image resolution may be improved by removing the dependence on the emission PSF. This is particularly important in turbid specimens in which the scattered fluorescence signal is not confined in a single pixel of the CCD imager and may degrade the image resolution.

Simultaneous Two-Photon Fluorescence and Reflected-Light Confocal Microscopy

Imaging light scattering in biological specimens, due to changes in refractive index, can also yield important structural information not shown in fluorescent images. As such, confocal reflected light and two-photon fluorescence are complementary techniques that can allow different specimen structures to be visualized based on different contrast mechanisms. The capability of optical deep-tissue microscopy has been demonstrated by the simultaneous imaging of ex vivo human skin in

both two-photon fluorescence and reflected-light confocal modes (139). Complementary structures are clearly obtained by using either method in the basal layer (Figure 11), but TPE provides better visualization of collagen/elastin fibers in the dermis.

Integrating Fluorescence Spectroscopy into Two-Photon Microscopes

Fluorescence spectroscopy is a powerful method to assay biological structure and functions. Spectroscopy techniques based on probe emission wavelength, lifetime, and emission polarization have been developed. Wavelength-resolved probes have been designed to measure many cell characteristics such as metabolite concentrations. Two-photon microscopes are typically designed with multiple detection channels such that emission wavelength changes can be monitored. The polarization of fluorescence emission measures the changes in the excitation and emission dipole directions of the fluorophore. One of the most common applications is the characterization of rotational diffusion rate. A polarization-resolving TPM has been designed (152) and has been applied to study rotational diffusion of single molecules in organic glasses. Fluorescence lifetime measures the residence time of the fluorophore in the excited state. Lifetime-resolved two-photon microscopes have been developed based on frequency domain (29) and time domain (153, 154) methods. Fluorescence lifetime is often highly sensitive to the

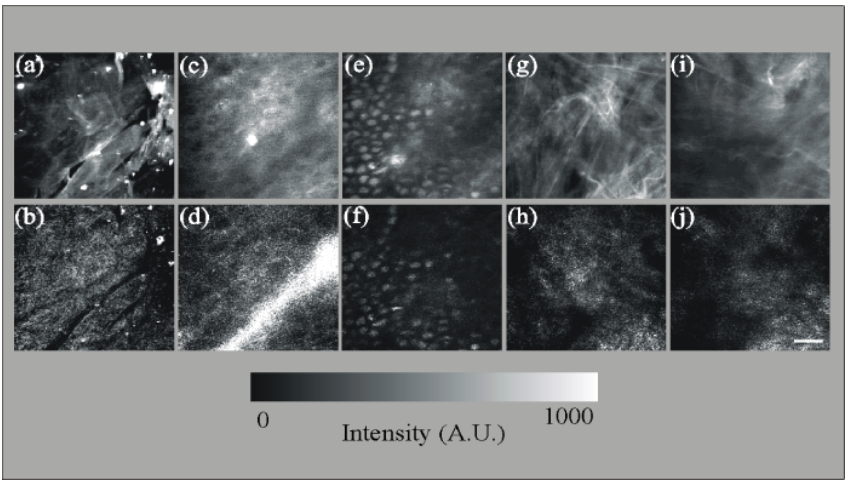

Figure 11 A comparison of two-photon fluorescence (*top panels*) and confocal reflected light images (*bottom panels*). Three-dimensional resolved structural layers were acquired from ex vivo human skin: (*a*, *b*) stratum corneum; (*c*, *d*) epidermis; (*e*, *f*) basal layer; (*g*, *h*, *i*, *j*) dermis. This figure is adapted from 66.

fluorophore biochemical microenvironment. Lifetime-sensitive functional probes have been identified for common applications such as Ca^{2+} or pH measurements, providing a complementary approach to wavelength-resolved measurement. It is more important that there are interesting processes that can be best measured by lifetime-resolved imaging. Examples include the determination of tissue oxygenation based on lifetime changes on oxygen quenching (155, 156). Another example includes the use of lifetime resolved measurement to quantitatively monitor the proteolytic process of antigenic materials in macrophage vacuoles (157, 158) (Figure 12; see color insert).

CONCLUSION

Within a decade after the invention of TPM, this technology has found applications in many diverse areas, ranging from the study of single molecules to tissue imaging. It is important that TPM is also starting to attract attention from the clinical and industrial communities. The development of a two-photon endoscope will be a critical step toward realizing noninvasive optical biopsy. As a complement to traditional pathology, the ability for a two-photon endoscope to rapidly and noninvasively acquire tissue-structural images may find use in areas such as surgical margin determination. TPM is also being applied by the pharmaceutical industry for high-throughput drug screening in which TPE or three-photon excitation of tryptophan or tryosine allows label-free study of protein-drug interactions. Highly sensitive two-photon FCS and PCH may be applied for further quantitative analysis. Given the importance of studying biological systems in vivo, we can project that the use of TPM in academic research will continue to increase. As two-photon technology reaches maturity, it is also promising that high-impact clinical and industrial applications may be identified.

ACKNOWLEDGMENTS

P. T. C. So acknowledges kind support from the National Science Foundation (MCB-9604382), National Institute of Health (R29GM56486-01), and American Cancer Society (RPG-98-058-01-CCE). C. Y. Dong acknowledges fellowship support from NIH 5F32CA75736-02.

LITERATURE CITED

1. Denk W, Strickler JH, Webb WW. 1990. Two-photon laser scanning fluorescence microscopy. *Science* 248:73–76
2. Williams RM, Piston DW, Webb WW. 1994. Two-photon molecular excitation provides intrinsic 3-dimensional resolution for laser-based microscopy and microphotochemistry. *FASEB J.* 8:804–13
3. Denk WJ, Piston DW, Webb WW. 1995. Two-photon molecular excitation laser-

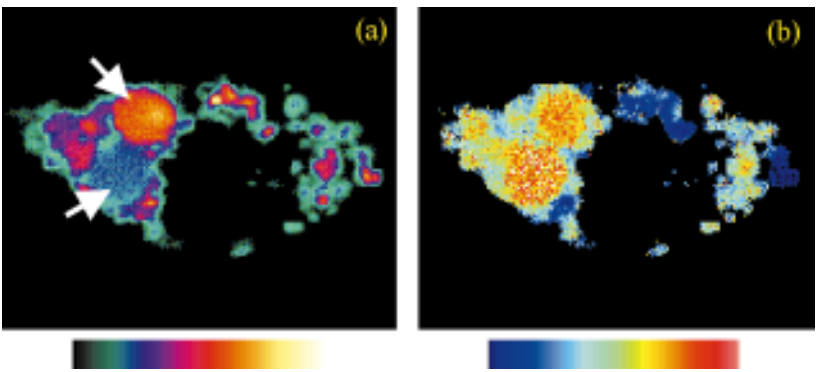

Figure 12 Fluorescence intensity and lifetime images of mouse macrophage cells after internalizing a proteolysis probe. The probe, bovine serum albumin labeled with fluorescein at a ratio of 1:15–22 is mostly non-fluorescent and has a short lifetime in its native form owing to self-quenching. After proteolysis, the protein fragments become highly fluorescent and have a long lifetime. With only intensity information, the stages of proteolysis in different vacuoles cannot be determined because the amount of probe in each vacuole is unknown. However, lifetime measurement is independent of the probe loading concentration and can provide an accurate measure of proteolysis progress. Note that the two large vacuoles (*arrows*) at the left side of the cell have very different intensities. It would be incorrect to conclude that the vacuoles are at different stages of proteolysis. The lifetime image indicates that both vacuoles have the same lifetime. Data and images are adapted from (158, 160).

scanning microscopy. In *Handbook of Biological Confocal Microscopy*, ed. JB Pawley, pp. 445–58. New York: Plenum
4. Hell SW. 1996. Nonlinear optical microscopy. *Bioimaging* 4:121–23
5. Denk WJ, Strickler JP, Webb WW. 1991. *US Patent No. 5034613*
6. Wilson T, Sheppard CJR. 1984. *Theory and Practice of Scanning Optical Microscopy*. New York: Academic. 213 pp.
7. Pawley JB, ed. 1995. *Handbook of Confocal Microscopy*. New York: Plenum. 632 pp.
8. Masters BR. 1996. *Selected Papers on Confocal Microscopy*. Bellingham, WA: SPIE. 702 pp.
9. Göppert-Mayer M. 1931. Uber elementarakte mit zwei quantensprungen. *Ann. Phys. (Leipzig)* 5:273–94
10. Franken PA, Hill AE, Peters CW, Weinreich G. 1961. Generation of optical harmonics. *Phys. Rev. Lett.* 7:118–19
11. Kaiser W, Garrett CGB. 1961. Two-photon excitation in CaF_2:Eu^{2+}. *Phys. Rev. Lett.* 7:229–31
12. McClain WM. 1971. Excited state symmetry assignment through polarized two-photon absorption studies in fluids. *J. Chem. Phys.* 55:2789
13. Friedrich DM, McClain WM. 1980. Two-photon molecular electronic spectroscopy. *Annu. Rev. Phys. Chem.* 31:559–77
14. Friedrich DM. 1982. Two-photon molecular spectroscopy. *J. Chem. Educ.* 59: 472
15. Birge RR. 1986. Two-photon spectroscopy of protein-bound fluorophores. *Acc. Chem. Res.* 19:138–46
16. Singh S, Bradley LT. 1964. Three-photon absorption in naphthalene crystals by laser excitation. *Phys. Rev. Lett.* 12:162–64
17. Rentzepis PM, Mitschele CJ, Saxman AC. 1970. Measurement of ultrashort laser pulses by three-photon fluorescence. *Appl. Phys. Lett.* 7:229–31
18. Gryczynski I, Szmacinski H, Lakowicz JR. 1995. On the possibility of calcium imaging using Indo-1 with three-photon excitation. *Photochem. Photobiol.* 62:804–8

18a. Freund I, Kopf L. 1970. Long Range Order in NH_4Cl. *Phys. Rev. Lett.* 24:1017–21

19. Hellwarth R, Christensen P. 1974. Nonlinear optical microscopic examination of structures in polycrystaline ZnSe. *Opt. Commun.* 12:318–22
20. Sheppard CJR, Kompfner R, Gannaway J, Walsh D. 1977. *The scanning harmonic optical microscope*. Presented at IEEE/OSA Conf. Laser Eng. Appl., Washington, DC
21. Gannaway JN, Sheppard CJR. 1978. Second harmonic imaging in the scanning optical microscope. *Opt. Quantum Electron.* 10:435–39
22. Barad Y, Eisenberg H, Horowitz M, Silberberg Y. 1997. Nonlinear scanning laser microscopy by third harmonic generation. *Appl. Phys. Lett.* 70:922–24
23. Squier JA, Muller M, Brakenhoff GJ, Wilson KR. 1998. Third harmonic generation microscopy. *Opt. Exp.* 3:315–24
24. Campagnola PJ, Wei M-D, Lewis A, Loew LM. 1999. High-resolution nonlinear optical imaging of live cells by second harmonic generation. *Biophys. J.* 77:3341–49
25. Baym G. 1974. *Lectures on Quantum Mechanics*. Menlo Park, CA: Benjamin/Cummins. 594 pp.
26. Callis PR. 1997. The theory of two-photon induced fluorescence anisotropy. In *Nonlinear and Two-Photon-Induced Fluorescence*, ed. J Lakowicz, pp. 1–42. New York: Plenum
27. Sheppard CJR, Gu M. 1990. Image formation in two-photon fluorescence microscope. *Optik* 86:104–6
28. Gu M, Sheppard CJR. 1995. Comparison of three-dimensional imaging properties between two-photon and single-photon fluorescence microscopy. *J. Microsc.* 177:128–37
29. So PTC, French T, Yu WM, Berland KM, Dong CY, Gratton E. 1995. Time-resolved fluorescence microscopy using two-photon excitation. *Bioimaging* 3:49–63

30. Diaspro A, Corosu M, Ramoino P, Robello M. 1999. Adapting a compact confocal microscope system to a two-photon excitation fluorescence imaging architecture. *Microsc. Res. Tech.* 47:196–205
31. Wokosin DL, Centonze VE, White J, Armstrong D, Robertson G, Ferguson AI. 1996. All-solid-state ultrafast lasers facilitate multiphoton excitation fluorescence imaging. *IEEE J. Sel. Top. Quantum Electron.* 2:1051–65
32. Hell SW, Booth M, Wilms S. 1998. Two-photon near- and far-field fluorescence microscopy with continuous-wave excitation. *Opt. Lett.* 23:1238–40
33. Centonze VE, White JG. 1998. Multiphoton excitation provides optical sections from deeper within scattering specimens than confocal imaging. *Biophys. J.* 75:2015–24
34. Gauderon R, Lukins RB, Sheppard CJR. 1999. Effects of a confocal pinhole in two-photon microscopy. *Microsc. Res. Tech.* 47:210–14
35. Xu C, Webb WW. 1997. Multiphoton excitation of molecular fluorophores and nonlinear laser microscopy. In *Nonlinear and Two-Photon-Induced Fluorescence*, ed. JR Lakowicz, pp. 471–540. New York: Plenum
36. Hermann JP, Ducuing J. 1972. Dispersion of the two-photon cross section in rhodamine dyes. *Opt. Commun.* 6:101–5
37. Xu C, Guild J, Webb WW, Denk W. 1995. Determination of absolute two-photon excitation cross sections by in situ second-order autocorrelation. *Opt. Lett.* 20:2372–74
38. Albota MA, Xu C, Webb WW. 1998. Two-photon fluorescence excitation cross sections of biomolecular probes from 690 to 960 nm. *Appl. Opt.* 37:7352–56
39. Lakowicz JR, Gryczynski I. 1992. Tryptophan fluorescence intensity and anisotropy decays of human serum albumin resulting from one-photon and two-photon excitation. *Biophys. Chem.* 45:1–6
40. Lakowicz JR, Kierdaszuk B, Callis P, Malak H, Gryczynski I. 1995. Fluorescence anisotropy of tyrosine using one- and two-photon excitation. *Biophys. Chem.* 56:263–71
41. Kierdaszuk B, Malak H, Gryczynski I, Callis P, Lakowicz JR. 1996. Fluorescence of reduced nicotinamides using one- and two-photon excitation. *Biophys. Chem.* 62:1–13
42. Chen ZP, Kaplan DL, Yang K, Kumar J, Marx KA, Tripathy SK. 1997. Two-photon-induced fluorescence from the phycoerythrin protein. *Appl. Opt.* 36:1655–59
43. Shear JB, Xu C, Webb WW. 1997. Multiphoton-excited visible emission by serotonin solutions. *Photochem. Photobiol.* 65:931–36
44. Chalfie M, Tu Y, Euskirchen G, Ward WW, Prasher DC. 1994. Green fluorescent protein as a marker for gene expression. *Science* 263:802–5
45. Niswender KD, Blackman SM, Rohde L, Magnuson MA, Piston DW. 1995. Quantitative imaging of green fluorescent protein in cultured cells: comparison of microscopic techniques, use in fusion proteins and detection limits. *J. Microsc.* 180:109–16
46. Potter SM, Wang CM, Garrity PA, Fraser SE. 1996. Intravital imaging of green fluorescent protein using two-photon laser-scanning microscopy. *Gene* 173:25–31
47. Masters BR, Chance B. 1999. Redox confocal imaging: intrinsic fluorescent probes of cellular metabolism. In *Fluorescent and Luminescent Probes for Biological Activity*, ed. WT Mason, pp. 361–74. London: Academic
48. Piston DW, Masters BR, Webb WW. 1995. Three-dimensionally resolved NAD(P)H cellular metabolic redox imaging of the in situ cornea with two-photon excitation laser scanning microscopy. *J. Microsc.* 178:20–27
49. Masters BR, So PTC, Gratton E. 1997. Multiphoton excitation fluorescence microscopy and spectroscopy of in vivo human skin. *Biophys. J.* 72:2405–12

50. Wang X, Krebs LJ, Al-Nuri M, Pudavar HE, Ghosal S, et al. 1999. A chemically labeled cytotoxic agent: two-photon fluorophore for optical tracking of cellular pathway in chemotherapy. *Proc. Natl. Acad. Sci. USA* 96:11081–84
51. Gryczynski I, Gryczynski Z, Lakowicz JR, Yang D, Burke TG. 1999. Fluorescence spectral properties of the anticancer drug topotecan by steady-state and frequency domain fluorometry with one-photon and multi-photon excitation. *Photochem. Photobiol.* 69:421–28
52. Albota M, Beljonne D, Bredas J-L, Ehrlich JE, Fu J-Y, et al. 1998. Design of organic molecules with large two-photon absorption cross sections. *Science* 281:1653–56
53. Mohler WA, Simske JS, Williams-Masson EM, Hardin JD, White JG. 1998. Dynamics and ultrastructure of developmental cell fusions in the Caenorhabditis elegans hypodermis. *Curr. Biol.* 8:1087–90
54. Mohler WA, White JG. 1998. Stereo-4-D reconstruction and animation from living fluorescent specimens. *BioTechniques* 24:1006–12
55. Squirrell JM, Wokosin DL, White JG, Bavister BD. 1999. Long-term two-photon fluorescence imaging of mammalian embryos without compromising viability. *Nat. Biotechnol.* 17:763–67
56. Keyse SM, Tyrrell RM. 1990. Induction of the heme oxygenase gene in human skin fibroblasts by hydrogen peroxide and UVA (365 nm) radiation: evidence for the involvement of the hydroxyl radical. *Carcinogenesis* 11:787–91
57. Tyrrell RM, Keyse SM. 1990. New trends in photobiology: the interaction of UVA radiation with cultured cells. *J. Photochem. Photobiol. B* 4:349–61
58. Konig K, So PTC, Mantulin WW, Tromberg BJ, Gratton E. 1996. Two-photon excited lifetime imaging of autofluorescence in cells during UVA and NIR photostress. *J. Microsc.* 183:197–204
59. Konig K, Becker TW, Fischer P, Riemann I, Halbhuber K-J. 1999. Pulse-length dependence of cellular response to intense near-infrared laser pulses in multiphoton microscopes. *Opt. Lett.* 24:113–15
60. Sako Y, Sekihata A, Yanagisawa Y, Yamamoto M, Shimada Y, et al. 1997. Comparison of two-photon excitation laser scanning microscopy with UV-confocal laser scanning microscopy in three-dimensional calcium imaging using the fluorescence indicator Indo-1. *J. Microsc.* 185:9–20
61. Koester HJ, Baur D, Uhl R, Hell SW. 1999. Ca^{2+} fluorescence imaging with pico- and femtosecond two-photon excitation: signal and photodamage. *Biophys. J.* 77:2226–36
62. Hockberger PE, Skimina TA, Centonze VE, Lavin C, Chu S, et al. 1999. Activation of flavin-containing oxidases underlies light-induced production of H_2O_2 in mammalian cells. *Proc. Natl. Acad. Sci. USA* 96:6255–60
63. Schonle A, Hell SW. 1998. Heating by absorption in the focus of an objective lens. *Opt. Lett.* 23:325–27
64. Jacques SL, McAuliffe DJ, Blank IH, Parrish JA. 1987. Controlled removal of human stratum corneum by pulsed laser. *J. Invest. Dermatol.* 88:88–93
65. Pustovalov VK. 1995. Initiation of explosive boiling and optical breakdown as a result of the action of laser pulses on melanosome in pigmented biotissues. *Kvantovaya Elektron.* 22:1091–94
66. Buehler C, Kim KH, Dong CY, Masters BR, So PTC. 1999. Innovations in two-photon deep tissue microscopy. *IEEE Eng. Med. Biol. Mag.* 18:23–30
67. Nie SM, Zare RN. 1997. Optical detection of single molecules. *Annu. Rev. Biophys. Biomol. Struct.* 26:567–96
68. Ambrose WP, Goodwin PM, Jett JH, Orden AV, Werner JH, Keller RA. 1999. Single molecule fluorescence spectroscopy at ambient temperature. *Chem. Rev.* 99:2929–56

69. Weiss S. 1999. Fluorescence spectroscopy of single biomolecules. *Science* 283:1676–83
70. Xie XS, Lu HP. 1999. Single-molecule enzymology. *J. Biol. Chem.* 274:15967–70
71. Mertz J, Xu C, Webb WW. 1995. Single-molecule detection by two-photon-excited fluorescence. *Opt. Lett.* 20:2532–34
72. Overway KS, Duhachek SD, Loeffelmann K, Zugel SA, Lytle FE. 1996. Blank-free two-photon excited fluorescence detection. *Appl. Spectrosc.* 50:1335–37
73. Brand L, Eggeling C, Seidel CAM. 1997. Single-molecule detection of coumarin-120. *Nucleosides Nucleotides* 16:551–56
74. Song JM, Inoue T, Kawazumi H, Ogawa T. 1998. Single molecule detection by laser two-photon excited fluorescence in a capillary flowing cell. *Anal. Sci.* 14:913–16
75. Hanninen PE, Soini JT, Soini E. 1999. Photon-burst analysis in two-photon fluorescence excitation flow cytometry. *Cytometry* 36:183–88
76. Van Orden A, Cai H, Goodwin PM, Keller RA. 1999. Efficient detection of single DNA fragments in flowing sample streams by two-photon fluorescence excitation. *Anal. Chem.* 71:2108–16
77. Plakhotnik T, Walser D, Pirotta M, Renn A, Wild UP. 1996. Nonlinear spectroscopy on a single quantum system: two-photon absorption of a single molecule. *Science* 271:1703–5
78. Walser D, Plakhotnik T, Renn A, Wild UP. 1997. One- and two-photon spectroscopy on single molecules of diphenyloctatetraene. *Chem. Phys. Lett.* 270:16–22
79. Xu C, Shear JB, Webb WW. 1997. Hyper-Rayleigh and hyper-Raman scattering background of liquid water in two-photon excited fluorescence detection. *Anal. Chem.* 69:1285–87
80. Sanchez EJ, Novotny L, Holtom GR, Xie XS. 1997. Room-temperature fluorescence imaging and spectroscopy of single molecules by two-photon excitation. *J. Phys. Chem. A* 101:7019–23
81. Lewis MK, Wolanin P, Gafni A, Steel DG. 1998. Near-field scanning optical microscopy of single molecules by femtosecond two-photon excitation. *Opt. Lett.* 23:1111–13
82. Schwille P, Korlach J, Webb WW. 1999. Fluorescence correlation spectroscopy with single-molecule sensitivity on cell and model membranes. *Cytometry* 36: 176–82
83. Schwille P, Haupts U, Maiti S, Webb WW. 1999. Molecular dynamics in living cells observed by fluorescence correlation spectroscopy with one- and two-photon excitation. *Biophys. J.* 77:2251–65
84. Bhawalkar JD, He GS, Park C-K, Zhao CF, Ruland G, Prasad PN. 1996. Efficient, two-photon pumped green upconverted cavity lasing in a new dye. *Opt. Commun.* 124:33–37
85. Bopp MA, Jia Y, Haran G, Morlino EA, Hochstrasser RM. 1998. Single-molecule spectroscopy with 27 fs pulses: time-resolved experiments and direct imaging of orientational distributions. *Appl. Phys. Lett.* 73:7–9
86. Sonnleitner M, Schutz GJ, Schmidt T. 1999. Imaging individual molecules by two-photon excitation. *Chem. Phys. Lett.* 300:221–26
87. Kirsch AK, Subramaniam V, Striker G, Schnetter C, Arndt-Jovin DJ, Jovin TM. 1998. Continuous wave two-photon scanning near-field optical microscopy. *Biophys. J.* 75:1513–21
88. Zenhausern F, O'Boyle MP, Wickramasinghe HK. 1994. Apertureless near-field optical microscope. *Appl. Phys. Lett.* 65: 1623–25
89. Novotny L, Sanchez EJ, Xie XS. 1998. Near-field optical imaging using metal tips illuminated by higher-order Hermite-Gaussian beams. *Ultramicroscopy* 71:21–29
90. Kawata Y, Xu C, Denk W. 1999. Feasibility of molecular-resolution fluorescence near-field microscopy using multi-photon

absorption and field enhancement near a sharp tip. *J. Appl. Phys.* 85:1294–301

91. Sanchez EJ, Novotny L, Xie XS. 1999. Near-field fluorescence microscopy based on two-photon excitation with metal tips. *Phys. Rev. Lett.* 82:4014–17
92. Magde D, Elson E, Webb WW. 1972. Thermodynamic fluctuations in a reacting system: measurement by fluorescence correlation spectroscopy. *Phys. Rev. Lett.* 29:705–8
93. Thompson NL. 1991. Fluorescence correlation spectroscopy. In *Topics in Fluorescence Spectroscopy*, ed. JR Lakowicz, pp. 337–78. New York: Plenum
94. Berland KM, So PTC, Gratton E. 1995. Two-photon fluorescence correlation spectroscopy: method and application to the intracellular environment. *Biophys. J.* 68:694–701
95. Berland KM, So PTC, Chen Y, Mantulin WW, Gratton E. 1996. Scanning two-photon fluctuation correlation spectroscopy: particle counting measurements for detection of molecular aggregation. *Biophys. J.* 71:410–20
96. Chen Y, Muller JD, Berland KM, Gratton E. 1999. Fluorescence fluctuation spectroscopy. *Methods Companion Methods Enzymol.* 19:234–52
97. Chen Y, Muller JD, So PTC, Gratton E. 1999. The photon counting histogram in fluorescence fluctuation spectroscopy. *Biophys. J.* 77:553–67
98. Inoue S, Spring KR. 1997. *Video Microscopy: The Fundamentals*. New York: Plenum. 741 pp.
99. Koutalos Y. 1999. Intracellular spreading of second messengers. *J. Physiol.* 519(3):629
100. Szmacinski H, Gryczynski I, Lakowicz JR. 1993. Calcium-dependent fluorescence lifetimes of Indo-1 for one- and two-photon excitation of fluorescence. *Photochem. Photobiol.* 58:341–45
101. Brust-Mascher I, Webb WW. 1998. Calcium waves induced by large voltage pulses in fish keratocytes. *Biophys. J.* 75:1669–78
102. Denk W, Holt JR, Shepherd GM, Corey DP. 1995. Calcium imaging of single stereocilia in hair cells: localization of transduction channels at both ends of tip links. *Neuron* 15:1311–21
103. Yu WM, So PTC, French T, Gratton E. 1996. Fluorescence generalized polarization of cell membranes: a two-photon scanning microscopy approach. *Biophys. J.* 70:626–36
104. Parasassi T, Gratton E, Zajicek H, Levi M, Yu W. 1999. Detecting membrane lipid microdomains by two-photon fluorescence microscopy. *IEEE Eng. Med. Biol. Mag.* 18:92–99
105. Bagatolli LA, Gratton E. 1999. Two-photon fluorescence microscopy observation of shape changes at the phase transition in phospholipid giant unilamellar vesicles. *Biophys. J.* 77:2090–101
106. Maiti S, Shear JB, Williams RM, Zipfel WR, Webb WW. 1997. Measuring serotonin distribution in live cells with three-photon excitation. *Science* 275:530–32
107. Xu C, Zipfel W, Shear JB, Williams RM, Webb WW. 1996. Multiphoton fluorescence excitation: new spectral windows for biological nonlinear microscopy. *Proc. Natl. Acad. Sci. USA* 93: 10763–68
108. Denk W. 1994. Two-photon scanning photochemical microscopy: mapping ligand-gated ion channel distributions. *Proc. Natl. Acad. Sci. USA* 91:6629–33
109. Pettit DL, Wang SS, Gee KR, Augustine GJ. 1997. Chemical two-photon uncaging: a novel approach to mapping glutamate receptors. *Neuron* 19:465–71
110. Furuta T, Wang SS, Dantzker JL, Dore TM, Bybee WJ, et al. 1999. Brominated 7-hydroxycoumarin-4-ylmethyls: photolabile protecting groups with biologically useful cross-sections for two photon photolysis. *Proc. Natl. Acad. Sci. USA* 96:1193–200

111. Jaconi M, Pyle J, Bortolon R, Ou J, Clapham D. 1997. Calcium release and influx colocalize to the endoplasmic reticulum. *Curr. Biol.* 7:599–602
112. Lipp P, Niggli E. 1998. Fundamental calcium release events revealed by two-photon excitation photolysis of caged calcium in guinea pig cardiac myocytes. *J. Physiol.* 508:801–9
113. Brown EB, Webb WW. 1998. Two-photon activation of caged calcium with submicron, submillisecond resolution. *Methods Enzymol.* 291:356–80
114. Soeller C, Cannell MB. 1999. Two-photon microscopy: imaging in scattering samples and three-dimensionally resolved flash photolysis. *Microsc. Res. Tech.* 47:182–95
115. DelPrincipe F, Egger M, Ellis-Davies GC, Niggli E. 1999. Two-photon and UV-laser flash photolysis of the Ca^{2+} cage, dimethoxynitrophenyl-EGTA-4. *Cell Calcium* 25:85–91
116. Brown EB, Shear JB, Adams SR, Tsien RY, Webb WW. 1999. Photolysis of caged calcium in femtoliter volumes using two-photon excitation. *Biophys. J.* 76:489–99
117. Brown EB, Wu ES, Zipfel W, Webb WW. 1999. Measurement of molecular diffusion in solution by multiphoton fluorescence photobleaching recovery. *Biophys. J.* 77:2837–49
118. Denk W, Detwiler PB. 1999. Optical recording of light-evoked calcium signals in the functionally intact retina. *Proc. Natl. Acad. Sci. USA* 96:7035–40
119. Masters BR, So PTC, Gratton E. 1998. Optical biopsy of in vivo human skin: multi-photon excitation microscopy. *Lasers Med. Sci.* 13:196–203
120. So PTC, Kim H, Kochevar IE. 1998. Two-photon deep tissue ex vivo imaging of mouse dermal and subcutaneous structures. *Opt. Exp.* 3:339–50
121. Riegler M, Castagliuolo I, So PTC, Lotz M, Wang C, et al. 1999. Effects of substance P on human colonic mucosa in vitro. *Am. J. Physiol.* 276:G1473–83
122. Bennett BD, Jetton TL, Ying G, Magnuson MA, Piston DW. 1996. Quantitative subcellular imaging of glucose metabolism within intact pancreatic islets. *J. Biol. Chem.* 271:3647–51
123. Piston DW, Knobel SM, Postic C, Shelton KD, Magnuson MA. 1999. Adenovirus-mediated knockout of a conditional glucokinase gene in isolated pancreatic islets reveals an essential role for proximal metabolic coupling events in glucose-stimulated insulin secretion. *J. Biol. Chem.* 274:1000–4
124. Fetcho JR, O'Malley DM. 1997. Imaging neuronal networks in behaving animals. *Curr. Opin. Neurobiol.* 7:832–38
125. Denk W, Delaney KR, Gelperin A, Kleinfeld D, Strowbridge BW, et al. 1994. Anatomical and functional imaging of neurons using 2-photon laser scanning microscopy. *J. Neurosci. Methods* 54: 151–62
126. Yuste R, Denk W. 1995. Dendritic spines as basic functional units of neuronal integration. *Nature* 375:682–84
127. Yuste R, Majewska A, Cash SS, Denk W. 1999. Mechanisms of calcium influx into hippocampal spines: heterogeneity among spines, coincidence detection by NMDA receptors, and optical quantal analysis. *J. Neurosci.* 19:1976–87
128. Denk W, Sugimori M, Llinas R. 1995. Two types of calcium response limited to single spines in cerebellar Purkinje cells. *Proc. Natl. Acad. Sci. USA* 92:8279–82
129. Svoboda K, Denk W, Kleinfeld D, Tank DW. 1997. In vivo dendritic calcium dynamics in neocortical pyramidal neurons. *Nature* 385:161–65
130. Svoboda K, Helmchen F, Denk W, Tank DW. 1999. Spread of dendritic excitation in layer 2/3 pyramidal neurons in rat barrel cortex in vivo. *Nat. Neurosci.* 2:65–73
131. Helmchen F, Svoboda K, Denk W, Tank DW. 1999. In vivo dendritic calcium

dynamics in deep-layer cortical pyramidal neurons. *Nat. Neurosci.* 2:989–96

132. Shi SH, Hayashi Y, Petralia RS, Zaman SH, Wenthold RJ, et al. 1999. Rapid spine delivery and redistribution of AMPA receptors after synaptic NMDA receptor activation. *Science* 284:1811–16
133. Mainen ZF, Malinow R, Svoboda K. 1999. Synaptic calcium transients in single spines indicate that NMDA receptors are not saturated. *Nature* 399:151–55
134. Maletic-Savatic M, Malinow R, Svoboda K. 1999. Rapid dendritic morphogenesis in CA1 hippocampal dendrites induced by synaptic activity. *Science* 283:1923–27
135. Engert F, Bonhoeffer T. 1999. Dendritic spine changes associated with hippocampal long-term synaptic plasticity. *Nature* 399:66–70
136. Kleinfeld D, Mitra PP, Helmchen F, Denk W. 1998. Fluctuations and stimulus-induced changes in blood flow observed in individual capillaries in layers 2 through 4 of rat neocortex. *Proc. Natl. Acad. Sci. USA* 95:15741–46
137. Jones KT, Soeller C, Cannell MB. 1998. The passage of Ca^{2+} and fluorescent markers between the sperm and egg after fusion in the mouse. *Development* 125: 4627–35
138. Summers RG, Piston DW, Harris KM, Morrill JB. 1996. The orientation of first cleavage in the sea urchin embryo, Lytechinus variegatus, does not specify the axes of bilateral symmetry. *Dev. Biol.* 175:177–83
139. Kim KH, So PTC, Kochevar IE, Masters BR, Gratton E. 1998. Two-photon fluroescence and confocal reflected light imaging of thick tissue structures. *SPIE Proc.* 3260:46–57
140. Dabbs T, Glass M. 1992. Fiber-optic confocal microscopy: FOCON. *Appl. Opt.* 31:3030–35
141. Giniunas L, Justkaitis R, Shatalin SV. 1993. Endoscope with optical sectioning capability. *Appl. Opt.* 32:2888–90
142. Bhawalkar JD, Kumar ND, Zhao CF, Prasad PN. 1997. Two-photon photodynamic therapy. *J. Clin. Laser Med. Surg.* 15:201–4
143. Bodaness RS, Heller DF, Krasinski J, King DS. 1986. The two-photon laser-induced fluorescence of the tumor-localizing photosensitizer hematoporphyrin derivative: Resonance-enhanced 750 nm two-photon excitation into the near-UV Soret band. *J. Biol. Chem.* 261: 12098–101
144. Fisher WG, Partridge WP Jr, Dees C, Wachter EA. 1997. Simultaneous two-photon activation of type-I photodynamic therapy agents. *Photochem. Photobiol.* 66:141–55
145. Guild JB, Webb WW. 1995. Line scanning microscopy with two-photon fluorescence excitation. *Biophys. J.* 68:A290
146. Brakenhoff GJ, Squier J, Norris T, Bliton AC, Wade WH, Athey B. 1996. Real-time two-photon confocal microscopy using a femtosecond, amplified Ti:Sapphire system. *J. Microsc.* 181:253–59
147. Bewersdorf J, Pick R, Hell SW. 1998. Mulitfocal multiphoton microscopy. *Opt. Lett.* 23:655–57
148. Buist AH, Muller M, Squire J, Brakenhoff GJ. 1998. Real time two-photon absorption microscopy using multi point excitation. *J. Microsc.* 192:217–26
149. Petran M, Hadravsky M, Egger MD, Galambos R. 1958. Tandem scanning reflected light microscope. *J. Opt. Soc. Am.* 58:661–64
150. Fan GY, Fujisaki H, Miyawaki A, Tsay RK, Tsien RY, Ellisman MH. 1999. Video-rate scanning two-photon excitation fluorescence microscopy and ratio imaging with cameleons. *Biophys. J.* 76: 2412–20
151. Kim KH, Buehler C, So PTC. 1999. High-speed, two-photon scanning microscope. *Appl. Opt.* 38:6004–9
152. Farrer RA, Previte MJR, Olson CE, Peyser LA, Fourkas JT, So PTC. 1999.

Single-molecule detection with a two-photon fluorescence microscope with fast-scanning capabilities and polarization sensitivity. *Opt. Lett.* 24:1832–34

153. Straub M, Hell SW. 1998. Fluorescence lifetime three-dimensional microscopy with picosecond precision using a multifocal multiphoton microscope. *Appl. Phys. Lett.* 73:1769–71
154. Sytsma J, Vroom JM, de Grauw CJ, Gerritsen HC. 1998. Time-gated fluorescence lifetime imaging and microvolume spectroscopy using two-photon excitation. *J. Microsc.* 191:39–51
155. Helmlinger G, Yuan F, Dellian M, Jain RK. 1997. Interstitial pH and pO2 gradients in solid tumors in vivo: high-resolution measurements reveal a lack of correlation. *Nat. Med.* 3:177–82
156. Roh HD, Boucher Y, Kalnicki S, Buchsbaum R, Bloomer WD, Jain RK. 1991. Interstitial hypertension in carcinoma of uterine cervix in patients: possible correlation with tumor oxygenation and radiation response. *Cancer Res.* 51:6695–98
157. Weaver DJ Jr, Cherukuri A, Carrero J, Coelho-Sampaio T, Durack G, Voss EW Jr. 1996. Macrophage mediated processing of an exogenous antigenic fluorescent probe: time-dependent elucidation of the processing pathway. *Biol. Cell.* 87:95–104
158. French T, So PTC, Weaver DJ Jr, Coelho-Sampaio T, Gratton E, et al. 1997. Two-photon fluorescence lifetime imaging microscopy of macrophage-mediated antigen processing. *J. Microsc.* 185:339–53
159. Masters BR, So PTC. 1999. Multi-photon excitation microscopy and confocal microscopy imaging of in vivo human skin: a comparison. *Microsc. Microanal.* 5: 282–89
160. So PTC, Konig K, Berland K, Dong CY, French T, et al. 1998. New time-resolved techniques in two-photon microscopy. *Cell Mol. Biol.* 44:771–93
161. Xu C, Webb WW. 1996. Measurement of two-photon excitation cross sections of molecular fluorophores with data from 690 to 1050 nm. *J. Opt. Soc. Am. B* 13: 481–91

Annual Review of Biomedical Engineering
Volume 2, 2000

CONTENTS

PIERRE M. GALLETTI: A Personal Reflection, *Robert M. Nerem* 1

PHYSICOCHEMICAL FOUNDATIONS AND STRUCTURAL DESIGN OF HYDROGELS IN MEDICINE AND BIOLOGY, *N. A. Peppas, Y. Huang, M. Torres-Lugo, J. H. Ward, J. Zhang* 9

BIOENGINEERING MODELS OF CELL SIGNALING, *Anand R. Asthagiri, Douglas A. Lauffenburger* 31

FUNDAMENTALS OF IMPACT BIOMECHANICS: Part I - Biomechanics of the Head, Neck, and Thorax, *Albert I. King* 55

INJURY AND REPAIR OF LIGAMENTS AND TENDONS, *Savio L.-Y. Woo, Richard E. Debski, Jennifer Zeminski, Steven D. Abramowitch, Serena S. Chan Saw, MS, James A. Fenwick* 83

ELECTROPHYSIOLOGICAL MODELING OF CARDIAC VENTRICULAR FUNCTION: From Cell to Organ, *R. L. Winslow, D. F. Scollan, A. Holmes, C. K. Yung, J. Zhang, M. S. Jafri* 119

CRYOSURGERY, *Boris Rubinsky* 157

CELL MECHANICS: Mechanical Response, Cell Adhesion, and Molecular Deformation, *Cheng Zhu, Gang Bao, Ning Wang* 189

MICROENGINEERING OF CELLULAR INTERACTIONS, *Albert Folch, Mehmet Toner* 227

QUANTITATIVE MEASUREMENT AND PREDICTION OF BIOPHYSICAL RESPONSE DURING FREEZING IN TISSUES, *John C. Bischof* 257

MICROFABRICATED MICRONEEDLES FOR GENE AND DRUG DELIVERY, *Devin V. McAllister, Mark G. Allen, Mark R. Prausnitz* 289

CURRENT METHODS IN MEDICAL IMAGE SEGMENTATION, *Dzung L. Pham, Chenyang Xu, Jerry L. Prince* 315

ANTIBODY ENGINEERING, *Jennifer Maynard, George Georgiou* 339

NEW CURRENTS IN ELECTRICAL STIMULATION OF EXCITABLE TISSUES, *Peter J. Basser, Bradley J. Roth* 377

TWO-PHOTON EXCITATION FLUORESCENCE MICROSCOPY, *Peter T. C. So, Chen Y. Dong, Barry R. Masters, Keith M. Berland* 399

IMAGING THREE-DIMENSIONAL CARDIAC FUNCTION, *W. G. O'Dell, A. D. McCulloch* 431

THREE-DIMENSIONAL ULTRASOUND IMAGING, *Aaron Fenster, Donal B. Downey* 457

BIOPHYSICAL INJURY MECHANISMS IN ELECTRICAL SHOCK TRAUMA, *Raphael C. Lee, Dajun Zhang, Jurgen Hannig* 477

WAVELETS IN TEMPORAL AND SPATIAL PROCESSING OF BIOMEDICAL IMAGES, *Andrew F. Laine* 511

MICRODEVICES IN MEDICINE, *Dennis L. Polla, Arthur G. Erdman, William P. Robbins, David T. Markus, Jorge Diaz-Diaz, Raed Rizq, Yunwoo Nam, Hui Tao Brickner, Amy Wang, Peter Krulevitch* 551

NEUROENGINEERING MODELS OF BRAIN DISEASE, *Leif H. Finkel* 577

EXTRACORPOREAL TISSUE ENGINEERED LIVER-ASSIST DEVICES, *Emmanouhl S. Tzanakakis, Donavon J. Hess, Timothy D. Sielaff, Wei-Shou Hu* 607

MAGNETIC RESONANCE STUDIES OF BRAIN FUNCTION AND NEUROCHEMISTRY, *Kâmil Ugurbil, Gregor Adriany, Peter Andersen, Wei Chen, Rolf Gruetter, Xiaoping Hu, Hellmut Merkle, Dae-Shik Kim, Seong-Gi Kim, John Strupp, Xiao Hong Zhu, Seiji Ogawa* 633

INTERVENTIONAL AND INTRAOPERATIVE MAGNETIC RESONANCE IMAGING, *J. Kettenbach, D. F. Kacher, S. K. Koskinen, Stuart G. Silverman, A. Nabavi, Dave Gering, Clare M. C. Tempany, R. B. Schwartz, R. Kikinis, P. M. Black, F. A. Jolesz* 661

CARTILAGE TISSUE REMODELING IN RESPONSE TO MECHANICAL FORCES, *Alan J. Grodzinsky, Marc E. Levenston, Moonsoo Jin, Eliot H. Frank* 691

IN VIVO NEAR-INFRARED SPECTROSCOPY, *Peter Rolfe* 715